PREDICTING AIR TEMPERATURES IN CITY STREETS ON THE BASIS OF MEASURED REFERENCE DATA

A thesis submitted to The University of Adelaide in fulfilment of the requirements for a degree of Doctor of Philosophy

Evyatar Erell

The School of Architecture, Landscape Architecture and Urban Design

February 2005

CHAPTER 1: INTRODUCTION

"And yet I have constructed in my mind a model city from which all cities can be deduced," Kublai said. "It contains everything corresponding to the norm. Since the cities that exist diverge in varying degree from the norm, I need only foresee the exceptions to the norm and calculate the most probable combinations."

Italo Calvino, "Invisible Cities"

1.1 Overview: Application of urban climate research to the design of cities

Research on urban microclimate developed as a distinct specialisation once it became apparent that meteorological conditions in cities often differed substantially from conditions in rural areas. The ultimate benefit to be gained from understanding the microclimate of cities lies in the ability to respond to it in such a way as to create better environments for humans – a growing majority of whom now live in urban centres. This broad goal consists of dealing with two types of spaces - indoor (building) and outdoor (urban) - although Page (1968), an early pioneer of urban climatology, identified no less than 12 separate facets of urban design that were sensitive to climate. These include recognized problems such as optimisation of land-use patterns with respect to atmospheric pollution zoning, but also less-known goals such as adaptation of building form and site planning with respect to microclimatic modifications that affect both building performance and the comfort and utility of urban spaces. Oke (1984) noted that in order to be relevant to the planning process, studies of urban climatology needed both "an ability to demonstrate the importance of climate information in the design of settlements", and "the predictive power to foretell the climatic impact of alternative design strategies". In the ensuing years, concepts such as the 'urban heat island' have become increasingly familiar to the general public, but Page's (1968) observation that the planning profession lacked the tools to forecast the microclimate of the built environment from the properties of a green-field site is still valid, for the most part.

An early goal of several urban climate models was to create a set of data for input into building thermal analysis software that would describe conditions at a specific site more accurately than data from a reference station for the whole metropolitan area (Taha, 1978; El Nahas, 1996). There seems to be a clear case for the widespread use of such models, but there is currently no software expressly designed for this purpose. Many

building simulation software packages even come with inbuilt climate data files compiled from 'representative' stations such as airports. The error introduced in the use of generic climate data is unknown.

The design of outdoor spaces requires an understanding of the local environment. This has traditionally been the role of architects, who have relied on intuition, on personal experience and on the examples of others. For instance, a study of the indigenous architecture of the cold desert of Leh and hot desert of Jaisalmer (Krishan, 1996) included numerous observations regarding appropriate design strategies for such climates. A study of the indigenous towns of Algeria combined with an analysis of solar angles led to the recommendation that solar access be restricted to elevations of 60-70 degrees or more, by means of controlling the street width and the use of cantilevered balconies (Mazouz and Zerouala, 1998; Mazouz, 1999). The ancient town planners of the Middle East have often been credited with a superior understanding of the environment, suggesting that there were lessons to be learned for modern planners (Rahamimoff and Bornstein, 1981; Potchter, 1990-91).

Urban climatologists too have attempted to apply theoretical insights in order to influence real-world planning. Oke (1984) found a number of shortcomings in microclimate research that prevented it from becoming an applied science, including a lack of quantitative techniques and relationships; lack of standardization, generality and transferability; and the absence of clear guidelines for those wishing to learn and use climatological principles in settlement planning. He identified several research topics that could help bridge the gap, and later carried out an analysis of the effect of street aspect ratio on various meteorological parameters, coming to the conclusion that a height to width ratio (H/W) of 0.4 was an appropriate geometrical guideline for the design of mid-latitude cities (Oke, 1988a).

An attempt to synthesize generalized rules and guidelines that may be of value to urban designers in different climates was carried out at the behest of the World Meteorological Organization (Givoni, 1989). It contains a broad overview of the state of the art of published research by planners and microclimatologists, and prescriptions for urban design in a variety of climates, but lacks generalized quantitative tools to assist in the resolution of real-world design problems in specific conditions.

Traditionally, climatological information is given to planners in the form of tables, diagrams or maps of variables such as air temperature, relative humidity or solar radiation – all of which give a static description of certain properties of the climate, singly or in combination (e.g. Olgyay's bioclimatic chart). Such data may be directly applicable in some cases, such as rainfall statistics required for the design of storm sewers. However, in general, the relevance is not obvious since climatic data are difficult to translate into technical requirements in the planning of cities or the design of buildings. The consequences of failing to account properly for environmental factors may be reflected in the economic costs of providing thermal comfort, but they also affect human health and general well-being in ways that are more difficult to quantify. This shortcoming reflects a real gap between climatology and its application. Taesler (1984) proposed that integrated 'input-output' models, describing climatic conditions and their impact on various elements of the urban 'system,'

might bridge this gap. Any model to be useful must reflect reality, must be predictive and should allow comparison of alternative urban designs on the basis of predetermined criteria.

Although sustained research in urban climatology is over fifty years old, there are still very few examples of this knowledge being applied in a systematic manner in the design of urban space (Mills, 1999). This is partly due to differences in methodology between architects and climatologists. Architectural environmental research focuses on the relationship between humans and their surroundings; it is guided by an empirical and inferential approach; and it tends to present results as guidelines. Urban climatologists, on the other hand, deal with abstract phenomena such as the nocturnal urban heat island that may have little bearing on human thermal comfort; employ an experimental approach that often seeks to isolate the phenomenon being studied; and present the results in the context of general meteorological studies with often little thought of practical application.

1.2 Definition of problem and research questions

Analysis of the environmental conditions in a given region forms the basis of climate-conscious design of the built environment. Climatic factors should be considered at all scales of the planning process, ranging from the creation of master plans for whole metropolitan areas to the design of individual buildings. In responding to questions on the effect of climate on the thermal performance of buildings, a basic difficulty arises: The variety of conditions found within the urban environment is the result, to a great extent, of the spatial organization and material structure of its component parts. This has two implications:

- Decisions made in the urban planning process may result in localized modification of the climatic conditions in various parts of the city. However, there is presently no simple tool available to planners to assess these changes while still in the planning stage, before construction begins. Current research in urban climatology is mostly theoretical in nature, seeking to understand and quantify the basic processes that affect the built environment. Most computerized models are research tools designed to investigate issues of general scientific interest, and are not intended to provide architects and town planners with a means of simulating the effect of specific design strategies.
- At the scale of the individual building, there are a number of computer models aimed at simulating thermal performance and associated energy consumption. The models range from rudimentary tools developed for the early design stage to extremely complex and very detailed models for HVAC design. However, all of these models have one requirement in common – they require input of ambient environmental conditions. These are generally based upon data monitored over extended periods of time at a small number of standard stations, generally one for each city, which rarely reflect the conditions found in city-centre locations. However, these data are nonetheless used as the basis for the environmental analysis carried out when designing buildings, regardless of the fact that they may result in substantial errors.

There is thus a need for a method of providing site-specific meteorological data that represent a closer approximation of reality than data from regional meteorological stations. Such data may provide a useful guide to urban planners wishing to assess the effect of town planning strategies, and allow more accurate simulation of the thermal performance of individual buildings.

This research project is aimed at developing a computer model that can be used to predict air temperature in a specific urban location on the basis of meteorological data from a reference site for which data is available. It builds to a certain extent on previous work by El Nahas (1996), but takes a different path on several key issues. The challenge is to combine and codify published studies of the basic individual thermodynamic processes that occur in the urban canopy layer so as to produce an integrated model of air temperature that reflects all of the geometric and material factors that affect its evolution at a given point over time. The success of the project is determined to a great extent by the accuracy of the prediction and the confidence in the model's ability to handle a wide range of environmental conditions.

1.3 Research objectives

The main objectives of this research are to:

a) Collect accurate and well-documented hourly meteorological measurements for an extended period from several urban sites and a reference station, for use in this project and which may be used in other studies of the urban climate as well.

b) Develop and validate a computer model capable of predicting site-specific air temperature in a city street for extended periods, with simplified inputs based on climate data from a reference station in the region.

Specifically, the research seeks to establish whether a relatively simple uncoupled model of the temperature in the urban canopy, i.e. a model in which there is no feedback from the micro-scale site to the meso-scale urban boundary layer, can predict the temperature at a given site with sufficient accuracy to be a useful tool for simulating the relationship between urban form and site-specific air temperature.

1.4 Significance of the problem

Human settlement is becoming increasingly urbanized in all countries. The number of urban dwellers has risen from about 600 million in 1890 to about 2 billion in 1986 (Santamouris, 1998). In the developed countries, including Australia, 90 percent or more of the population live in cities, and urbanization is continuing unabated in the less developed countries, too. The number of urban agglomerations with a population exceeding one million residents is over 360 worldwide (United Nations - Department of Economic and Social Affairs, 2003). On current trends, about 80 percent of the world's population will be living in cities by the end of the twenty first century. Clearly, all aspects of the urban environment have a bearing on the lives of an increasing proportion of mankind, so our understanding of conditions in the city is of great importance.

Urbanization has usually been accompanied first by industrialization and a degradation of the environment, followed by economic development and a rapidly improving standard of living. This improvement relies to a great extent on intensive use of non-renewable energy for the operation of equipment, and increasingly for space conditioning (cooling and heating) as well. However, the production and consumption of energy using currently available technology have long-term environmental effects on a global scale, such as contributing to the build up of greenhouse gases in the atmosphere. They are also responsible for altering the environment of cities, contributing directly to the urban heat island effect and indirectly because dense urban construction, especially high-rise buildings, cannot be operated without energy intensive equipment.

Growing public awareness of environmental issues has resulted in renewed interest in measures to conserve energy and in the design of climatically responsive buildings and urban spaces. The benefits of climate-responsive design include very large savings of energy over the entire life cycle of buildings, beginning with reduced capital costs for equipment and including lower operating costs. To achieve these goals, architects, planners and engineers employ computer-aided design in a variety of applications. Many of these require an accurate description of the environment, including site-specific meteorological conditions. The lack of sufficiently accurate data can lead to substantial errors in the calculation of energy consumption of buildings. By providing meteorological information that is more accurate than that obtained from monitoring stations that are typically located a substantial distance away from building sites, this research contributes to the global effort to conserve energy and to improve the quality of the human environment.

1.5 Methodology

The research was carried out in three phases:

a) An extensive literature survey was carried out to investigate state-of-the art research on the basic physical processes that contribute to the urban microclimate. The survey placed particular emphasis on quantitative models and parameterisation schemes that could form part of a simplified modelling framework for predicting air temperature in an urban street canyon.

b) A database was created of environmental data representing conditions at a number of sites in central Adelaide and at a reference site with no buildings in the immediate surroundings. The meteorological records used to validate the model of air temperature in the urban canopy were assembled from meteorological data collection stations that were established at several sites in the city of Adelaide. Data from sites in urban canyons in the densely built central part of the city were compared with records from a reference station at a site where conditions are as close as possible to the natural environment of the region and which show a minimum urban effect from the surrounding metropolitan area.

c) A model was developed to predict air temperature in an urban canyon from measured data in a reference weather station, and implemented in a computer code (CAT). It was validated by comparing predicted temperatures with measured ones, analysing errors and systematically evaluating the effect of individual components of the software, making adaptations, additions and corrections as necessary.

1.6 Organization of thesis

The thesis begins with a literature review of the state of the art in research on urban climatology, incorporated in Chapter 2. The review includes sections on the various processes known to have an effect on the urban microclimate, and has a separate section on the application of climatology to urban planning.

Chapter 3 describes the theoretical basis of the urban climate model, which includes several parameterisation schemes to quantify the effect of various mechanisms on the micro-scale environment of the urban street canyon.

Chapter 4 describes the field study that was conducted with the aim of monitoring meteorological conditions at several sites in central Adelaide. In general, complete confidence in the capabilities of any model requires extensive field studies under a variety of environmental conditions in a fully representative sample of building configurations. Such a task was beyond the scope of this research, which was limited in resources. However, the meteorological records obtained in this study contributed to a rigorous test of the model's validity in the limited conditions studied, and were essential to its development.

Data assembled during the field study were analysed in Chapter 5 to highlight the diversity of air temperature in the study area. The differences in air temperature were correlated with a variety of other meteorological parameters, such as wind speed, wind direction, cloud cover and atmospheric humidity to establish significant relationships over the course of almost an entire year.

The calibration and validation of the CAT model are described in Chapter 6. The computer model was initialised with standard values of the parameterisation schemes, and a sensitivity analysis was carried out to test the effect of the constituent inputs on the quality of the predictions, using measured temperature data in an urban street canyon as the basis for comparison. Refinement and improvement of the computer program were undertaken in response to the contribution of the various components to errors in the predicted values. The model in its final form was then evaluated by running it on a different set of input data and measuring its performance by means of various statistical measures to establish its validity and define the range of environments to which it is applicable.

The thesis concludes with a discussion of possible applications of the model, as well as its limitations. Chapter 7 also incorporates a demonstration of the effect of running a simulation of the thermal performance of a building using input data modified by CAT, in comparison with a simulation carried out with input data that do not take into account micro-scale climatic modifications in the city. Finally, directions for future research are outlined that may build upon progress achieved in this project.

CHAPTER 2: URBAN MODIFICATIONS TO METEOROLOGICAL CONDITIONS NEAR THE SURFACE

The effect of buildings on microclimatic conditions in their vicinity, as well as on their interior, is one of the primary reasons for their construction. Therefore, "the placement of a building on the landscape gives rise to radiative, thermal, moisture and aerodynamic modification of the surrounding environment" (Oke, 1987). The environmental effect of placing a large number of buildings in close proximity, as in a city, is due not only to the sum of the effects of the individual buildings, but also to the complex interactions between them. The cumulative effect of human activities in cities on micro-climatic conditions was already evident in Roman times, where urban pollution was commented upon by Seneca (Landsberg, 1981). The first systematic study of the urban climate, as such, was probably conducted by Luke Howard, who identified an urban heat island in London as early as 1820 (Landsberg, 1981). The climate of London again served as the basis for another landmark study of urban climatology (Chandler, 1965), which incorporated meteorological data from eighteen standard meteorological stations in the Greater London area, supplemented by data from more limited stations and from mobile (vehicle) traverses. The wide-ranging study found substantial variations not only in air temperature but also in humidity, occurrence of fog and duration of sunshine, which were attributed to anthropogenic sources of heat and air pollution.

The discipline has since evolved into a distinct branch of meteorology. Lowry (1967) gave a popularised description of the mechanisms leading to the creation of a distinct urban climate, and a decade later enough research had accumulated on the subject to produce an extensive book (Landsberg, 1981). The urban heat island (UHI) has since become one of the most well-known manifestations of the urban climate, and has been documented thoroughly in recent years on the basis of detailed studies of meteorological data from networks of stations in and around cities of various sizes in different climates - Vancouver (Runnals and Oke, 1998); Tel Aviv (Saaroni *et al.*, 2000); Melbourne (Morris and Simmonds, 2001); Seoul (Kim and Baik, 2002); Athens (Livada *et al.,* 2002); and New York City (Gedzelman *et al.,* 2003), to mention a few. A weak urban heat island was even recorded in humid, tropical Singapore (Goh and Chang, 1999). The development of an UHI when a new city is founded on a greenfield site was monitored by Landsberg and Maisel (1972), who reported that over a period of three years, a heat island of up to 4.5^{o}C appeared as the newly established town of Columbia, Maryland grew to a population of 10,000 residents. Analyses of long-term temperature records in several locations - Turkey (Tayanc and Toros, 1997); Alaska (Magee *et al*., 1999); Athens (Philandras *et al.,* 1999); South Korea (Choi *et al.,* 2003); and North America (Engelhart and Douglas, 2003) – show an increase in the urban heat island effect parallelling increasing urbanisation.

Differences between the city and the rural surroundings occur on two distinct scales (Oke, 1976): The *urban canopy layer* consists of air contained between the urban roughness elements, typically buildings. Its climate is dominated by the nature of the immediate surroundings, especially site materials and geometry. The *urban boundary layer* is that portion of the planetary boundary layer whose characteristics are affected by the presence of an urban area at its lowest boundary, generally considered to be approximately at roof level, and is affected by processes occurring over a meso-scale area.

Figure 2. 1: Schematic depiction of the urban atmosphere interface illustrating a two-layer classification of urban modification (*Oke, 1976*).

The present research is limited to processes occurring within the urban canopy layer, and does not extend to issues such as the suppression of rain by atmospheric air pollution from urban or industrial sources, a phenomenon that has regional or possibly even global effects (Rosenfeld, 2000). It is mostly concerned with air temperature in the urban canopy layer, or more specifically, in an idealised section - the urban canyon. This has been considered the primary element of the urban matrix since it was first proposed that in order to understand the urban climate in general it was necessary to study in detail the exchanges taking place near the complex urban surface (Nunez and Oke, 1977). Figure 2.2 below illustrates what has become the conventional depiction of the urban canyon, and the heat exchange processes occurring within it.

The following review will, however, encompass all aspects of urban climatology, in order to shed some light on the processes affecting the urban canyon and to establish the conceptual background for the study.

Early quantitative studies of the urban microclimate proposed a heat balance equation as the framework incorporating the different factors acting upon it (Fuggle and Oke, 1970):

$$Q^* + Q_F = Q_H + Q_E + Q_S + Q_A \qquad (2.1.)$$

where Q^* is the net all-wave radiation, Q_F is anthropogenic heat, Q_H turbulent (sensible) heat exchange by convection, Q_E latent heat transfer, Q_S net storage and Q_A net advected energy. (Note: The original notation has been changed to reflect current conventions.)

Figure 2.2: **Schematic depiction of a) the urban/atmosphere interface, including an urban canyon and the enclosed volume of air (dashed); and b) sensible heat exchanges into and out of the canyon air volume *(Nunez and Oke, 1977)*.**

Differences between the urban climate and rural conditions with respect to each of these terms will serve as a framework for the review. A separate section will be devoted to the effects of vegetation: while it plays a part in most of the above mechanisms, it will be analysed separately in view of the complexity of its role. The review will conclude with a section on deliberate human modifications to the urban microclimate.

2.1 Radiation balance

The radiative exchanges occurring over any outdoor surface may be described by the balance equation formulated by Fuggle and Oke (1970), adapted to current notation:

$$Q^* = (K_{dir} + K_{dif})(1-\alpha) + L\downarrow - L\uparrow \qquad (2.2.)$$

where Q^* is the net radiative balance, K_{dir} direct beam short wave (solar radiation), K_{dif} diffuse solar radiation, α the albedo of the surface and $L\uparrow$ and $L\downarrow$ the long wave radiation emitted by the surface and received by it from the sky, respectively.

Urbanization affects the absorption of incoming (mostly) short-wave solar radiation as well as the emission of long wave infrared radiation from the surface. This is due to the combined effects of urban morphology, which results in interference with the transmission of radiant energy, to differences in the surface properties of man-made materials and to air pollution.

Short wave (solar) radiation

Solar radiation received at the surface of the earth is the main source of energy in the urban canopy layer. The geometry of the city affects the absorption of this radiation in complex ways. Terjung and Louie (1973) realised that the mutual shading of tall buildings in a dense urban fabric could result in two seemingly contradictory phenomena: While multiple reflections of the sun's rays on building surfaces result in greater absorption overall compared to a flat horizontal surface, the amount of solar radiation penetrating to the street level is lower. The 'solar heat island' was found to be strongest in high-latitude cities, but was also predicted to occur (to a lesser extent) in equatorial cities, where solar elevation is higher.

The proportion of energy reflected from the urban surface, and thus not affecting conditions in the canopy layer, is determined at two levels:

a. For a photon of light striking a terrestrial surface, the probability of being reflected is determined by the angle of incidence and by the wavelength-weighted and spatially averaged reflectivity of solar radiation (referred to as albedo). The albedo of typical urban surfaces may vary from only 0.05 for dark asphalt to 0.8 for whitewashed roofs (Oke, 1987).

b. The albedo of a city as a whole is affected by the reflectivity of individual surfaces, but also by the morphology of the urban area. Certain configurations of buildings lead to an increased probability of multiple reflections in the canopy layer, resulting in a low urban albedo.

Studies to assess the range of typical values for urban albedo have been carried out by several methods – analytical, scale-model and empirical, with somewhat varying results.

Application of a detailed numerical model of radiation exchange to the city of Columbus, Ohio, showed that all urban areas reflect less incoming solar radiation than adjacent rural areas (Arnfield, 1982). Accordingly, typical values for solar reflectivity were found to be in the range of 0.18-0.21 for low-rise residential areas, compared with only 0.07-0.14 for dense high-rise commercial districts. (Albedo for rural areas that are covered with vegetation is reported as being in the range of 0.2-0.25). The model, which takes into account properties of building and paving materials, the morphology of typical buildings and the orientation of the streets, and analyses both direct solar radiation and diffuse radiation from the sky also indicates that average reflectivity decreases as solar altitude increases, so lower values are predicted for midday compared with early morning or late afternoon. Similarly, predicted urban albedo is higher in winter than in summer.

A more recent numerical model based on the photon-tracking method (Kondo et al., 2001) produced substantially higher values, generally in the range 0.3-0.4, but is also an interesting attempt to correlate albedo with urban morphology. The study evaluated the effect of four factors:

- Building coverage
- Canopy height
- Orientation of roads
- Building height distribution

Albedo was found to decrease with increasing building height and decreasing uniformity of height. The model predicted a relatively high albedo in very dense configurations, due to reflection off roof surfaces, and in very low-density urban forms, because of reflections from road surfaces. The orientation of roads, while having obvious local effects, was not found to have clear-cut effects on an urban scale. Finally, the study suggests that albedo is always relatively high when solar altitude is high, regardless of building coverage. In contrast, another recent computer model finds that albedo is highest in the morning and afternoon, because low solar elevation results in greater reflection from rooftops, whereas trapping inside the canyons becomes the dominant mechanism when the sun is near the zenith (Chimklai et al., 2004).

The effect of morphology on the albedo of a city has also been investigated by means of a scale model consisting of cubic concrete blocks 0.15m a side placed on the roof of a building (Aida, 1982). Results of this experiment suggested that annual albedo for a city located at 35 degrees latitude could vary between 0.23 and 0.4. A numerical model developed following this experiment (Aida and Gotoh, 1982) found that the maximum absorption occurs when the canyon width is approximately twice the block width. Soler and Ruiz (1994) confirmed this finding in an empirical study comparing the intensity of reflected radiation in satellite images of urban and rural areas near Barcelona with terrestrial measurements. Reduction in albedo was found to be greatest in medium density neighbourhoods. It was also proposed that in dense areas, a large proportion of incoming solar radiation is reflected at roof level, and the effect of multiple reflections in the urban canyon is proportionately smaller.

It is worth noting that the albedo measured by Aida using the simplified urban configurations is substantially higher than empirical values for real urban sites investigated by several researchers (Sailor and Fan, 2002). Characteristic urban surface albedo based on remote-sensing data reported in numerous studies is within a range of 0.09-0.27, with a mean value of approximately 0.14 for urban centres (Oke, 1988b). Rural values are typically higher by about 0.05, probably because dark coloured roofing materials and the trapping role exerted by urban geometry result in less reflection compared with typical rural surfaces (Aida, 1982). There are, however, large disparities among cities and between different neighbourhoods of the same city. Taha (1997) noted that most US and European cities had an albedo in the range 0.15-0.20, whereas some North African towns had an albedo as high as 0.30-0.45. Regardless of these apparent disparities, Arnfield used these data to validate his own model (Arnfield, 1988) – which likewise predicts a much higher albedo for the simplified urban configurations modelled than is reported in various empirical studies. The empirical values reported by Soler and Ruiz – 0.22-0.23 - fall somewhere in between.

Table 2.1: Sample of albedo values assigned to various land use classifications by several researchers *(Sailor and Fan, 2002)*.

Sailor and Fan also proposed that while the reflectivity of most natural surfaces is almost independent of incidence angle (except for very acute angles solar zenith angles), the albedo of an urban area changes substantially with solar position. This is because the albedo of a city is not simply the area-weighted average of the albedo of individual surfaces, but is affected by the geometric relationship between surfaces such as walls, roofs and the ground. The paper introduces an 'energy weighted albedo' (EWA) that is a time-varying function of solar position. The 'nadir-view albedo' (NVA) used traditionally, which measures albedo from a fixed point directly above the city regardless of solar angle, typically has a single (i.e. constant) value, and underestimates daily solar radiative loads by 11-22%, depending on land use and urban morphology.

The albedo of an urban canyon (as distinct from the urban surface as a whole) was modelled to assess the effect of glazed surfaces typical of modern office construction (Tsangrassoulis and Santamouris, 2003). The albedo of relatively deep canyons (H/W>1) was found to be less than approximately 0.2 for typical construction materials with diffuse reflection (e.g. masonry), for a wide range of sun angles. Increasing the window-to-wall ratio resulted in a lower canyon albedo, because sunlight is transmitted by the glass to building interiors. In very deep canyons (H/W>2), the predicted albedo for all sun angles as well as for uniform diffuse radiation was between 0.01-0.03.

Long wave radiation

The relationship between the total hemispherical radiation emitted by a black body and its surface temperature is known as the Stefan-Boltzmann Law:

$$R^o = \sigma T^4 \qquad (2.3.)$$

where R^o is the total radiant energy in W m^{-2}, T is the absolute temperature in K and σ , known as the Stefan-Boltzmann constant, is 5.67 x 10^{-8} W m^{-2} K^{-4}.

The radiation given off by a real object may be calculated by introducing its total hemispherical emissivity, ε, which is, by definition, less than unity:

$$R = \varepsilon \sigma T^4 \qquad (2.4.)$$

The wavelength distribution of radiation emitted by a black body is given by Planck's Law:

$$R_\lambda^o(T) = \frac{C_1}{\lambda^5[e^{(C_2/\lambda T)} - 1]} \tag{2.5.}$$

where $R_\lambda^o(T)$ is the emittance at temperature T (K) for the wavelength λ(μm), and the constants are C_1 = 3.741 x 10^{-16} m^2 W and C_2 = 0.014388 m K.

This function approaches zero at very small and very large wavelengths. The wavelength at which a black body emits radiation with the highest intensity depends only on the temperature of the emitting surface, and may be calculated from Wien's Displacement Law, as follows:

$$\lambda_{\max} \cdot T = 2897.8 \tag{2.6.}$$

where $\lambda_{\max}$ is the wavelength of maximum emission, in μm, and T the absolute temperature of the radiating surface (K).

The radiation incident on a body may be absorbed, reflected or transmitted through it. The fractions of the absorbed, reflected and transmitted radiation are called *absorptivity* (α), *reflectivity* (ρ) and *transmissivity* (τ), respectively. The sum of these fractions is, by definition, unity:

$$\alpha + \rho + \tau = 1 \tag{2.7.}$$

It should be noted that these values are total hemispherical values, and characterize the overall interaction between an object and the radiation impinging on it.

The relation between the emitting and absorbing properties of a body is given by Kirchoff's Law, which states that for every wavelength and for every direction of propagation, the directional spectral emissivity are equal to its directional spectral absorptivity:

$$\alpha_\lambda(T, \varphi, \theta) = \varepsilon_\lambda(T, \varphi, \theta) \tag{2.8.}$$

In assessing the *net radiative heat loss* from a terrestrial surface, (i.e. neglecting the effects of convection) the counter-radiation received from the sky, which is affected by atmospheric conditions, must also be taken into account.

The incoming atmospheric infrared radiation can be expressed in two ways:

1. The sky may be assumed to behave like a black body, with an emissivity of 1.0. In this case, the radiation given off by the sky is given by the expression:

$$R_{sky} = \sigma T_{sky}^4 \tag{2.9.}$$

which requires a means of calculating the apparent temperature of the sky (The apparent sky temperature at a particular location and time is defined as the temperature a black body would have in order to radiate the same amount of energy as that received from the sky by a horizontal radiator.);

or

2. The sky may be assumed to have a temperature equal to the ambient dry bulb temperature near the ground (T_a), in which case the differences in radiation emitted due to variations in atmospheric moisture content are accounted for by modifying the sky emissivity ε_{sky}:

$$R_{sky} = \sigma \varepsilon_{sky} T_a^4 \qquad (2.10.)$$

where T_a is the dry bulb temperature of the air near the ground, in K.

Both of these methods disregard the spectral distribution of the incoming sky radiation, and deal only with the total flux of radiant energy, assumed to have a continuous spectrum. These methods are applicable when the radiating surface approximates a black body, or is *grey body* - i.e. it absorbs all wavelengths indiscriminately. (Most natural materials are grey bodies, but several building materials, particularly polished metals, are spectrally selective, and have different emissivities in the long wave part of the spectrum and in the solar spectrum).

Incoming long wave radiation ($L\downarrow$) is not generally measured at meteorological stations. Various statistical correlations have therefore been proposed between $L\downarrow$ and meteorological parameters which are measured on a widespread basis and which may be used as surrogates for atmospheric emissivity. Some of these models of atmospheric emissivity are summarized in Table 2.2 (Oke, 1987).

Arnfield (1979) evaluated the accuracy of some of these expressions on the basis of independent empirical data. He suggested that the Swinbank (1963) and Idso and Jackson (1969) relations performed best, and since they require no calibration to local conditions they possess a high degree of spatial and temporal stability. The Brunt (1932) relation, on the other hand, requires *a priori* knowledge of local conditions for selection of appropriate regression coefficients. All expressions required correction for cloudy conditions (see below). However, the Idso and Jackson formula, with appropriate adjustment for cloud type and amount, gave good predictions of daily totals (albeit with variable accuracy on an hourly basis). An evaluation of eight parameterisation models, including all of the ones in Table 2.2 above except number 5, suggests that all of these schemes tend to underestimate incoming long wave radiation in very clear, cold clear weather by 20-60 W m^{-2} (Niemela et al., 2001). The study, based on measurements carried out in Finland, suggested different coefficients for two discrete ranges of e_0, but as its authors suggest, it is probably best suited to high-latitude locations.

Table 2.2: Formulae to calculate the atmospheric emissivity of clear skies ε_a *(Oke, 1987, p. 374).*

In the above models, the effect of altitude on long wave radiation at the surface is incorporated indirectly through its effect on air temperature and atmospheric moisture content. A recent model (Iziomon et al., 2003) proposes a parameterisation scheme in which the effects of altitude are incorporated in two empirical coefficients:

$$L\downarrow = \sigma T_a^{\,4}\{1 - x_s \exp(-Y_s e / T_a)\} \tag{2.11.}$$

The empirical parameters X_s and Y_s have values of 0.35 and 10 K hPa^{-1}, respectively, for lowland sites and values of 0.43 and 11.5 K hPa^{-1} for mountain sites. Vapour pressure e is measured in hPa.

Clouds have a strong influence upon long wave exchange in the atmosphere, because water has a very high absorptivity (and hence emissivity). Oke (1987) proposed the following modifications to the values for incoming sky radiation and for the net long wave radiation:

$$L\downarrow = L\downarrow_{(0)} (1 + an^2) \tag{2.12.}$$

$$L^* = L^*_{(0)} (1 - bn^2) \tag{2.13.}$$

where the constants 'a' and 'b' are a function of the cloud type (see Table 2.3), and 'n' is the fraction of the sky covered in cloud, expressed in tenths on a scale from zero to unity.

Table 2.3: Values of the coefficients used in equations 2.12 and 2.13 above to compensate for the effect of clouds on long wave radiation in the atmosphere *(Oke, 1987, p. 374)*

A simpler cloud correction function that does not require input of cloud characteristics was proposed by Martin (1989):

$$L\downarrow = (1 + 0.0224n - 0.0035n^2 + 0.00028n^3)L\downarrow_{clear} \quad (2.14.)$$

If the difference between the absolute temperatures of the surface and the sky is not large, the following linearized form of the Stefan-Boltzmann Law (Martin, 1989), may be used to relate the environmental conditions to the net radiative heat transfer at the surface:

$$R_{net} = 4\varepsilon\sigma T_a^3 (T_r - T_s) \quad (2.15.)$$

where R_{net} (W m^{-2}) is the net radiative heat loss, T_a (K) is the ambient air temperature, T_r (K) the radiator temperature and T_s (K) the equivalent sky temperature, and ε and σ are the emissivity and Stefan-Boltzmann constant, respectively.

Net radiative heat transfer may also be expressed by introducing a coefficient of radiant heat transfer at the surface. Setting this coefficient, h_r, to equal $4\varepsilon\sigma T_{air}^3$, equation 2.15 above then becomes

$$R_{net} = h_r\,(T_r - T_s) \quad (2.16.)$$

The value of h_r was determined experimentally (Oliveti et al., 2003) for a range of temperatures, and was found to vary within a fairly narrow range – about 3.9-6.5 W m^{-2} K. The typical diurnal range is on the order of 0.5 W m^{-2} K.

This section has thus far been concerned with the general physical principles governing radiant heat transfer. The following paragraphs trace the development of theories that explain the evolution of the nocturnal urban heat island on the basis of this mechanism.

Early empirical findings showed that the magnitude of the mid-latitude urban heat island was correlated with city size (Oke, 1973). However, the same studies also showed that the maximum urban-rural temperature difference occurred several hours after sunset on calm, cloudless nights[1], and is therefore largest when turbulent transfer is essentially absent and radiative exchange is restricted to the long wave band. This reasoning led to the proposition that a major cause of the nocturnal urban heat island is apparently the smaller sky view factor characteristic of dense urban centres, which results in reduced long wave heat loss. Nunez and Oke (1976) found that in calm, cloudless conditions, radiative exchange is the dominant mechanism controlling air temperature changes in an urban canyon. However, actual cooling rates were substantially lower than those reported in a study of above-roof conditions (Fuggle and Oke, 1976), especially during the second half of the night. Analysis of temperatures in a scale model subjected to strong radiative cooling showed that the nocturnal heat island in cities might result from obstruction of the sky by building surfaces (Oke, 1981). Maximum urban heat island intensities of up to 12 ^{o}C, which may occur at night in clear conditions with little wind, are thus attributed to the morphology of the city, typically measured by the canyon (urban street) sky view factor ψ_s. Field studies carried out in the suburbs of Tokyo confirmed the relationship between the minimum sky view factor of an urban area and the intensity of the UHI, even where the urban fabric was relatively sparse and the resulting temperature difference small (Yamashita et al., 1986). Oke (1998a) suggested that it may also be possible to predict actual UHI intensity based on the expression for maximum intensity, modified by appropriate factors to account for the effects of wind, cloud and rural moisture.

Once the importance of the relationship between the sky view factor of a location (generally denoted as 'SVF' or ψ_s) and radiant exchanges occurring in it was recognized, a number of methods were proposed to assist in its evaluation. These include a simplified graphical tool for calculating the wall view factor of a building, requiring as inputs the difference in azimuth between its ends and the angle of elevation of each of them (Watson and Johnson, 1987); a calculation method based on analysis of fish-eye lens photographs (Steyn, 1980; Steyn et al., 1986) and a method of automating this calculation procedure in the case of digital photographs (Grimmond et al., 1999; Grimmond et al., 2001)

The net long wave radiation balance is affected not only by the magnitude of the radiative flux emitted by terrestrial surfaces, but also by the magnitude of the incoming flux. Long wave radiation emitted by the sky is influenced primarily by the presence of atmospheric water vapour and clouds, but the temperature of the air itself also has a contribution. The increased warmth of the urban atmosphere compared to the rural one thus results in increased atmospheric counter-radiation over cities (Oke and Fuggle, 1972), though the net effect

[1] Most of the field studies on the urban heat island confirm that it is a nocturnal phenomenon. However, a number of studies also reported daytime heat islands: Chiang and Lo (1995) reported an urban heat island of about 5.5^{o}C in Taipei in the afternoon hours; Emmanuel (1997) found large daytime heat islands in Ann Arbor, Michigan, while Santamouris (1998) and Livada *et al*. (2002) reported a daytime heat island in Athens of up to 15^{o}C. Giridharan *et al.* (2004) also report a daytime heat island of about 1.5^{o}C in Hong Kong. This suggests that the daytime UHI is a phenomenon that occurs primarily in warm low-latitude cities.

of this process to the development of an urban microclimate is marginal. In a survey conducted in Goteborg, Sweden, (Nunez *et al.*, 1998) a maximum difference of only 17 W m^{-2} was observed between a rural site and the city centre, corresponding to only 5.7% reduction in incoming long wave radiation in the city. The same survey also found a corresponding increase in sky emissivity with increasing near-surface stability, i.e. it was larger over rural areas than over the city (in clear, calm weather). Sky emissivity measured over the city centre was about 0.79 compared to about 0.83 in rural areas.

An implicit but often ignored aspect of the mechanism responsible for the development of the nocturnal UHI is that the magnitude of the urban-rural difference is more sensitive to the rate of rural cooling than that of cooling in the city (Johnson et al., 1991). The UHI is relatively small when rural cooling rates are low, for instance in humid and overcast conditions. It is when rural cooling rates are high that the UHI is fully developed.

While canyon geometry, often represented by the sky view factor, has a great effect on radiant exchange in the city, its contribution to the urban heat island remains a complex issue. Barring *et al.* (1985) found high correlations between the SVF and surface temperatures in the streets of Malmo, measured with a hand-held thermal camera – but substantially lower correlations with air temperature in the same streets. Furthermore, while the maximum urban heat island measured in Malmo fitted in well with Oke's general relationship, the variations in air temperature along the streets were much smaller than variations in surface temperature. A possible explanation for this inconsistency is that micro-scale diversity in air temperature is reduced by advection, so that the temperature measured at a particular canyon reflects the spatially averaged energy balance in a larger urban area.

The effect of air pollution on air temperature in the city

Urban air pollution has a complex effect on radiation exchanges. Lowry (1967) recognised that the presence of aerosols in relatively high concentrations tends to reflect incoming solar radiation, and would thus be expected to lower daytime maximum temperatures. However, airborne particles also absorb outgoing long wave radiation, diminishing the potential for nocturnal cooling of terrestrial surfaces, and the reduction in incoming solar radiation (K↓) is also offset to a great degree by increased long wave radiation from the sky (L↓) (Arnfield, 1982). Urban-rural differences in levels of solar radiation attributed to air pollution in the form of aerosols varies widely from city to city (Arnfield, 1982). Various studies show an attenuation of up to 20%, but most research suggests that this value is usually less than 10%, since airborne particles tended to scatter direct radiation that is then received in the form of diffuse radiation (Oke, 1988b). Evidence for both effects has been found in temperature and radiation records for Mexico City, one of the largest and most polluted cities in the world (Jauregui and Luyando, 1999). As a result of air pollution, global radiation in this city may be reduced by as much as 25-35% relative to a rural site on clear days with low winds and high relative humidity. The studt also showed that daytime maximum temperatures have declined slightly in the suburbs over the past 25 years, but that in downtown areas the UHI dominates over the cooling effect of the aerosols.

At night radiative cooling was shown to have diminished, and the mean minimum temperatures have accordingly increased by nearly 2 °C over the same period.

2.2 Subsurface Energy Storage

Changes in air temperature near the ground are driven mainly by energy exchange at the surface. This in turn is affected by the thermal conductivity (k) and heat capacity ($C=\rho c$, where ρ is density and c specific heat) of the material. A parameter that combines these properties is the *thermal admittance* ($\mu=kC^{-1/2}$): materials with a high admittance absorb heat readily and transmit it to the substrate, only to release it easily when the ambient air becomes cooler. Such materials register a relatively small diurnal temperature change. Typical values of thermal admittance for both rural and urban surfaces vary over a wide range – from about 300 J m^{-2} $s^{1/2}$ K^{-1} for dry peat soil and foamed concrete to approximately 2500 J m^{-2} $s^{1/2}$ K^{-1} for wet sandy loam or dense concrete (Oke, 1981). While the thermal admittance undoubtedly has an effect on the surface temperature, and thus on the ambient air temperature, the complexity of the urban environment makes it very difficult to assess the overall effect of the differences between urban and rural materials. Swaid (1991) suggested that the net effect might be negligible, while Oke *et al.* (1991) found that the effect of differences in thermal admittance may be as large as that of radiative geometry, and that a 6 °C difference can be generated if μ_{rural} is very low. These apparently conflicting views may be resolved if one considers the effect of changes in soil moisture on the thermal properties on soil. Whereas the surface properties of urban areas are generally constant over time (with the exception of parks and gardens), changes in the rural environment, particularly soil moisture content, may be substantial (Oke, 1998b), and thus could have a dominant effect on the magnitude of the urban heat island. Ojima and Moriyama (1982) confirmed that (in a temperate climate such as Japan's), spatially averaged surface temperature was warmer in a city than in an adjacent rural area. Surveys with airborne infra-red sensors and detailed surface energy-budget models showed that in general, natural surfaces exhibited lower temperatures, higher latent heat flux and lower sensible heat flux than man-made surfaces. Similar results were reported by Oka *et al.* (1995), who found that sensible heat fluxes in urban areas were 40-100 W m^{-2} greater than in adjacent rural areas with the same net radiant balance, but that latent heat fluxes were 20-80 W m^{-2} smaller.

The process of energy storage is driven to a great extent by changes in the net radiant load. Early attempts to evaluate the size of the heat storage flux (ΔQ_S) assumed that it had a linear relationship to net radiation (Q^*). Oke *et al.* (1980/81) suggested that energy storage by different surface types could be characterised by coefficients giving the slope and offset of this relationship, but also suggested that different coefficients were necessary to describe daytime and night time heat exchange.

However, the proposition of a linear relationship between storage and net radiation does not explain the typical daily pattern of changes in the storage flux on sunny days: During the first third of the night ($Q^*<0$), urban surfaces release large amounts of heat stored during the daytime. This results in positive values of sensible heat (Q_H) even after net radiant exchange becomes negative, around sunset. Where radiant losses

to the sky are restricted by small sky view factors (as in dense urban canyons), the heat released from street surfaces is a major source of the urban heat island that typically forms at this time. In most urban locations, unlike rural areas, Q_H remains directed away from the surface throughout the night (Yap and Oke, 1974). Several hours after sunset, the radiative drain and the storage loss reach a balance. In the morning hours, when the net radiant load becomes positive again, the store is recharged (ΔQ_S>0). The atmosphere is usually relatively stable at this time, and sensible heat flux is small. In the afternoon, when the atmosphere is generally less stable, the coupling of the surface and atmosphere is better and turbulent heat flux into the air is more efficient.

The typical daily pattern of heat storage described above confirms a distinct phase lag between Q^* and ΔQ_S: Peak storage generally precedes maximum radiation levels by about 1-2 hours. Camuffo and Bernardi (1982), who noticed that storage was not simply a fraction of the net radiant flux incident upon the surface, proposed a hysteresis loop to describe storage flux in homogeneous ground surfaces:

$$\Delta Q_s = a_1 Q^* + a_2 \frac{\partial Q^*}{\partial t} + a_3 \qquad (2.17.)$$

where t is time; the parameter a_1 indicates the overall strength of the dependence of the storage heat flux on net radiation; a_2 determines whether the curves ΔQ_S and Q^* are exactly in phase (a_2=0), or ΔQ_S precedes Q^* (a_2>0); a_3 is the size of ΔQ_S when Q^* becomes negative: a large value of a_3 indicates that ΔQ_S becomes negative much earlier than Q^*. This equation was later verified by Oke and Cleugh (1987) for a variety of urban surfaces. Values of the coefficients a_1, a_2 and a_3 were derived empirically.

The above model describes heat storage in individual surfaces. Grimmond *et al.* (1991) used a similar formulation to describe the pattern of heat storage in a complex array of surfaces, characteristic of the three-dimensional urban surface. Each of the component surface types of a particular urban neighbourhood is weighted by its relative area, and the resulting values are summed for the area as a whole:

$$\Delta Q_s = \sum_{i=1}^{n} \{a_{1_i} Q^* + a_{2i} \frac{\partial Q^*}{\partial t} + a_{3i}\} \qquad (2.18.)$$

The model was found to be valid for daytime, when Q_F, the anthropogenic contribution to the energy balance, is relatively small compared to Q^*, the net radiative flux. At night, the anthropogenic flux may not always be neglected.

In order to be useful, the above model requires appropriate values of the coefficients a_1, a_2 and a_3 for each surface category. The urban canyon is one such surface type, but the heterogeneity of urban canyons in terms of orientation, aspect ratio etc. means that determination of appropriate values for these coefficients is not straightforward. Arnfield and Grimmond (1998) used an existing surface energy budget model (Arnfield, 1982) to manipulate various canyon properties, and used the results to assess the effects of these variations

on the coefficients of Grimmond's storage model. Compared to a 'standard' north-south canyon with equal walls and floor (5.6m), changing individual parameters yielded the following results:

- Canyon orientation has only a minor effect on overall energy stored, though the partitioning between different surfaces is affected.
- Increasing the aspect ratio (giving a deeper canyon) results not only in a large proportion of the net radiation being stored, but also in a greater lag between peak radiation and maximum storage rate.

The range of values obtained for the coefficients of the model is quite large, suggesting that the variations in the behaviour of individual canyons may be substantial. In the absence of net advection, and bearing in mind that the model does not treat latent heat, the thermal climate of neighbouring canyons may therefore be quite different.

Grimmond and Oke (2002) gave mean values for the coefficients of the objective hysteresis model (OHM) on the basis of empirical data from a number of sites, for several classes of surface types:

Table 2.4: Values of the coefficients used in the objective hysteresis model to describe storage heat flux in several classes of surface types *(Grimmond and Oke, 2002).*

Grimmond and Oke (1999c) determined the storage heat flux ΔQ_S in seven American cities as the energy-balance residual of direct observations of the net all-wave radiation, sensible heat and latent heat flux. While this method did not account for anthropogenic heat or the effects of convection, it nonetheless provides a useful framework for study. The storage flux was found to account for 17-58% of the daytime net radiation. When normalized by net all-wave radiation, storage heat flux was greater at urban sites, and less important at suburban sites where more extensive planted and irrigated surfaces resulted in a higher latent heat flux. ΔQ_S was found to fluctuate substantially over short periods of time, even under steady radiative forcing and uniform wind fetch, as the result of variability in the convective fluxes.

Sharlin and Hoffman (1984) proposed an alternative approach that evaluates the energy flux into the atmosphere from a surface as the sum of exponential decay terms of radiant energy absorbed over preceding time periods. At a certain depth below a surface, temperature remains constant over a typical diurnal cycle. The rate at which energy is dissipated at the surface is determined by its heat transfer coefficient and by the thermal properties of the material. This approach, which was the basis for a series of subsequent papers (Swaid, 1989; Swaid and Hoffman, 1990a; Swaid and Hoffman, 1990b; Swaid and

Hoffman, 1990c; Swaid, 1991; Swaid, 1993a; Swaid, 1995), described the propensity of a material to release stored energy by means of a 'time constant' (TC) that modified the basic exponential decay, and was expressed in the following generic form by Swaid (1991):

$$\Delta_{\lambda}[\Delta Q^{*}(\lambda)] = -\frac{\Delta Q^{*}(\lambda)}{h_c} \times \left[1 - \exp(-\frac{t-\lambda}{TC})\right] \qquad (2.19.)$$

where $\Delta\lambda$ is the difference between the air-surface temperature gradients during the time interval from t to λ in response to a change ΔQ^{*} in the net radiation on the surface and h_c is the convective surface heat transfer coefficient. The time constant is an attribute of the thermal inertia of the substrate. It is related (but not equal to) the thermal admittance μ.

The concept of a time constant was initially applied to prediction of the surface temperature of uniform materials (Swaid, 1989), and later to entire building clusters (in the form of the CTTC – the 'cluster thermal time constant'). The authors calculated typical values for the time constant on the basis of empirical measurements of the cooling rate of surfaces of common materials, with the following results (in hours): dry soil – 6.4; wet soil – 10.8; asphalt – 7.6; concrete – 9.6-10.5; and turf – 3.6 hours (Swaid, 1991).

Differences between urban and rural materials have been proposed as a possible mechanism for the creation of the urban heat island, since different materials exposed to the same environmental conditions may exhibit very dissimilar surface temperatures. Tan and Fwa (1992) reported not only the expected differences between planted surfaces and paved ones, but also substantial differences among different impervious materials. Paving materials such as granite slabs, terracotta bricks and interlocking concrete blocks displayed lower surface temperatures than asphalt at all times, especially in the late afternoon when sensible heat transfer to the air is largest. Asaeda *et al.* (1996) demonstrated that asphalt is indeed much warmer than bare soil during the daytime - but also found that the surface temperature of concrete pavement was similar to that of the soil. However, while much of the radiant energy absorbed in soil was released in the form of latent heat through evaporation of soil moisture, concrete and asphalt surfaces remained warmer at night and contributed substantial sensible fluxes to the urban atmosphere. Furthermore, they proposed that since most of the long wave radiation emitted by terrestrial surfaces is absorbed in the lowest 200 metres of the atmosphere, warm surfaces contributed directly to the boundary layer urban heat island directly even in the presence of strong thermal inversions suppressing turbulent exchange of sensible heat. In a night-time survey by concurrent airborne infra-red photography and measurement of screen level air temperature by vehicle traverse, Ben-Dor and Saaroni (1997) found that asphalt surfaces were the warmest elements of the urban matrix. Busy street intersections were found to be as much as 2 K warmer than adjacent streets, and it was speculated that this could be the result of friction with vehicle tires.

Luvall and Quattrochi (1998) proposed a method of classifying surfaces according to their response to net radiant load. Airborne thermal images taken at 30-minute intervals allowed calculation of a thermal response number (TRN), which was defined as the ratio between net radiant gain in the time interval and the change in

surface temperature. Moist soil and plants channel most of the radiant gain into latent heat, so their surface temperature shows little change, and hence have a higher TRN than most man-made surfaces. The technique has some descriptive value, but so far has no application in modelling.

2.3 Sensible heat flux

Sensible heat is transferred between the air and the adjacent urban surface when there is a temperature difference between them. The size of the convective component of the surface energy balance (Q_H) depends on two factors: The magnitude of the temperature difference, and the resistance to heat transfer between the surface and the adjacent air. The latter property is usually accounted for by its inverse, the convective heat transfer coefficient, so that the convective heat flux is given by the following expression:

$$Q_H = h_c\,(T_s - T_a) \tag{2.20.}$$

where Q_H is the rate of convective heat exchange (W m^{-2}), h_c is the convective heat transfer coefficient (W m^{-2} ^{o}C^{-1}), and T_s and T_a are the temperature of the surface and ambient air (^{o}C), respectively.

A variety of expressions for evaluating h_c have been proposed on the basis of empirical data:

Clark and Berdahl (1980) differentiated between three conditions (units converted to SI, h_c given in W m^{-2} ^{o}C^{-1}):

a) The radiating surface is colder than ambient air, and wind speed is low enough - (u < 0.076 m s^{-1}) - to allow free convection, i.e. the flow is laminar:

$$h_c = 0.8 \tag{2.21.}$$

b) The radiating surface is warmer than ambient air, and there is free convection (u < 0.45 m s^{-1}):

$$h_c = 3.5 \tag{2.22.}$$

c) Turbulent flow, regardless of the surface temperature (u greater than the values noted above for the relevant surface temperatures):

$$h_c = \frac{k(0.054Re^{0.8}Pr^{0.33})}{L} \tag{2.23.}$$

Clark and Berdahl note that the coefficient applied to the Reynolds number, 0.054, was increased above the smooth surface value (0.036), to account for surface roughness.

They also suggest that the following simplification of the relationship for turbulent flow is appropriate for wind speeds of 1.35-4.5 m s^{-1}:

$$h_c = 1.8V + 3.8 \tag{2.24.}$$

Where wind speeds are lower than 1.35 m s^{-1}, this expression overestimates the effects of convection.

Givoni (1982), summarizing Clark and Berdahl's findings, suggested a single formula that he claimed provides a reasonable representation of the convective coefficient over the wind speed range experienced in practice, when the surface temperature may be below ambient air dry bulb temperature:

$$h_c = 1 + 6\,V^{0.75} \qquad (2.25.)$$

where V is the wind speed (m s^{-1}).

Recent empirical evidence (Hagishima and Tanimoto, 2003) confirms the relationship between the convective surface heat exchange coefficient and wind speed in actual urban environments. They note, however, that due to the complexity of urban airflow, any such correlation can only be valid if it refers to wind speed very close to the surface in question – a distance of only 13 cm is suggested as a useful reference. The empirical correlations they proposed require a full three-dimensional characterisation of the wind. Such detailed information may in practice be available only from detailed computer modelling of airflow near the building.

The heterogeneous nature of the urban environment is difficult to characterise by means of a single representative temperature. However, although the surface energy balance is complex, any attempt to predict air temperature in the canopy layer requires an estimate of surface temperatures. Several experiments have been undertaken using airborne infrared sensors to investigate whether it was possible to measure such a value. Ben-Dor and Saaroni (1997) found a good correlation between surface temperatures measured by vehicle traverse and remotely-sensed surface temperatures measured concurrently. They proposed empirical regression coefficients resulting from their data, and suggested that these represent the effects of atmospheric humidity and of the characteristics of the equipment used. However, no attempt was made to test whether a generalized predictive relationship could be established on the basis of this data. Voogt and Oke (1997) defined a 'complete surface temperature' that takes into account the area-weighted temperature of all urban surfaces. Two methods were presented of obtaining this temperature, combining the use of airborne scans and ground traverses by vehicles. The complete surface temperature was found to differ substantially from remotely sensed estimates based on scans of the urban surface at different angles. Off-nadir observations from aerial sensors in the direction of the most shaded urban facet agreed most closely with this measure. The authors concluded, however, that there appears to be little utility in trying to estimate air temperature from remotely sensed surface temperature, of any kind.

The temperature of a surface may be calculated analytically, based on the thermal properties of the material such as conductivity, heat capacity and admittance, in addition to environmental factors such as radiant load, air temperature and wind speed. An alternative approach for this calculation that requires fewer inputs comprises a neural network model based on a backpropagation algorithm for the estimation of hourly values (Mihalakakou, 2002). The data-driven model requires 'training' using historic records of surface temperature and various environmental variables, but once calibrated is able to predict surface temperature using only readily available data for air temperature, relative humidity and global solar radiation.

The exchange of sensible heat depends, in addition to the heat transfer coefficient and surface temperature, discussed in the preceding paragraphs, on the temperature of air near the surface. Where terrain is flat and homogenous, air temperature near the surface is generally uniform. However, the urban canyon is a different case. Not only are surfaces not homogenous in material, solar exposure and orientation, but also the effect of geometry on airflow means that different surfaces may be exposed to different air velocities. Nakamura & Oke (1988) found that turbulent mixing tends to neutralize temperature gradients in the urban environment: the difference between air temperatures above and within the canyon was generally less than 1 °C – except within 0.5 m of wall surfaces. However, the same study found pockets of stagnant air (near the base of the walls) that remained undisturbed by the typical canyon vortex, where air temperature differences of up to 3 °C were observed.

The discussion in this section has dealt exclusively with sensible heat flux between ground (or building) surfaces and air immediately adjacent to them. The effects of turbulence on flux at greater elevations above the surface, for example at the interface between the canopy layer and the roughness sublayer above, will be discussed in section 2.5 below, which deals with the effects of the city on airflow.

2.4 Latent heat and the urban water balance

Evapotranspiration, the formation of dew and the urban water balance

The urban water budget for a volume comprising the urban canopy layer and the underlying soil to a depth where no net exchange of water takes place during the time period relevant to the process under examination can be written as

$$p + I + F = E + r + \Delta A + \Delta S \qquad (2.26.)$$

where p is precipitation, I is the piped water supply of the city, F is the water vapour released due to anthropogenic activities, such as combustion, E is evapotranspiration[2], r is runoff, ΔA is the net advection of moisture for the volume and ΔS is the change in water storage for the given period (Grimmond and Oke, 1991).The water balance is linked to the energy balance through the term E, which is the mass equivalent of the latent heat flux Q_E.

Grimmond *et al.* (1986) employed the balance equation above, with ΔA and F set to zero, to construct a model for the urban water balance, designed to be driven by standard climate data and employing simple, site-specific parameters. An important concept in this respect is the partitioning of the urban area into three types of surfaces from a hydroclimatic viewpoint:

[2] "Evapotranspiration (ET) is defined… as the physical process by which a liquid or solid is transferred to the gaseous state… The evaporation of water into the atmosphere occurs from the immediate surfaces of water bodies…from soils and from wet vegetation… The process of evaporation of water that has passed through the plant is called transpiration. Soil evaporation and plant transpiration occur simultaneously in nature, and there is no easy way to distinguish between the two processes. Therefore, the term evapotranspiration is used to describe the total process of water transfer into the atmosphere from vegetated land surfaces." (Rosenberg, 1974)

- Impervious surfaces, such as roads, parking lots and buildings. Such surfaces are either wet (saturated) immediately after rain, or dry.
- Pervious unirrigated, such as open untended park areas. Such surfaces may have a moisture status ranging anywhere from totally wet (saturated) to totally dry.
- Pervious irrigated, such as lawns and gardens, which are assumed to be always wet.

The availability of water is then calculated using conventional relations describing the hydrological properties of the surface and subsurface, including the retention capacity of the three types of surfaces and the soil storage capacity and field capacity of the pervious portion of the city.

Of special importance is the calculation of evapotranspiration, because of its effect on the urban energy balance. Grimmond *et al.* (1986) distinguished between two situations:

If the surface is wet or soil moisture is at field capacity, evaporation occurs at the potential rate, given by Priestly and Taylor (1972)

$$E = (\alpha/L_v)[s/(s+\gamma)](Q^*-\Delta Q_s) \qquad (2.27.)$$

where E is evapotranspiration, L_v is the latent heat of vaporisation, s is the slope of the saturation vapour pressure versus temperature relationship, γ is the psychrometric constant, Q^* is the net all-wave radiation flux density and ΔQ_s the subsurface heat flux density. α is the ratio of evaporation from a wet surface under conditions of minimal advection to the equilibrium evaporation, which is the lower limit to evaporation from moist surfaces. The value of α has been determined empirically, and is about 1.2-1.3 in suburban areas.

If the surface is moist or dry, evapotranspiration is restricted to a certain extent by water availability, and may be calculated by a modified version of Brutsaert and Stricker's (1979) advection-aridity equation:

$$E = (1/L_v)\left\{\left[(2\alpha-1)(s/s+\gamma))(Q^*-\Delta Q_s)\sum_{i=2}^{n} A_i\alpha_i'\right]-[AA(\gamma/(s+\gamma))E_a]\right\} \qquad (2.28.)$$

where A_i is the proportion of the catchment covered with the ith surface type, a'_i is an empirical coefficient of the *i*th surface type, defined as above, AA is the status of soil moisture related to area and E_a is refers to the drying power of the air:

$$E_a = (C/\gamma)(\overline{e}^* - \overline{e}_a)\left\{(\overline{u}/k^2)/[(\ln(z_v - d + z_{0v}/z_{0v}))\cdot\ln(z_u - d + z_{0m})/z_{om})]\right\} \qquad (2.29.)$$

where C is the heat capacity of dry air; $\overline{e}^*$ and $\overline{e}_a$ are the mean saturation and ambient vapour pressures at height z_v, respectively; u is the mean horizontal wind speed at height z_u; k is the von Karman constant (0.40); d is the zero-plane displacement length; and z_{0v} and z_{0m} are the water vapour and momentum roughness lengths, respectively.

Grimmond and Oke (1986) showed that even in temperate mid- and high-latitude cities (such as Vancouver, Canada), evapotranspiration may account for 30-70% of annual external water balance. Irrigation during the dry season helps to maintain high evapotranspiration rates, and has a substantial effect on the energy balance near the surface.

Formation and deposition of dew on terrestrial surfaces is the converse of evaporation, and may have equally substantial effects on energy exchange. While small in magnitude - dew accumulation is on the order of several tenths of a millimetre per night – dewfall is not a negligible term in the urban water balance. Furthermore, there are significant differences between dew formation on rural surfaces and on a variety of urban materials (Richards and Oke, 1998): Dewfall tends to be relatively abundant on grass or on low thermal mass surfaces in the city, such as exposed roof shingles, but tends to be absent from surfaces that stay warm throughout the night, such as pavement. Richards and Oke (1999) proposed a model to predict the formation of dew, incorporating thermal properties of the substrate in addition to weather conditions. However, the model does not provide a corresponding calculation of the energy released in the process, especially with regard to its partitioning between ground and atmosphere.

Partitioning energy between sensible and latent heat

In the absence of advection, surplus incoming energy not stored in the ground heats the air near the surface, increasing its sensible heat content, and evaporates surface water, if available, thus increasing the latent heat content of the air. If there is no moisture available, all of the surplus energy is converted to sensible heat, often resulting in a substantial rise in air temperature. The availability of water thus has a major effect on air temperature near the surface. Many impervious urban surfaces, such as asphalt roads, channel their entire net radiant surplus during the daytime into storage or into sensible heat, warming the substrate or the adjacent air. Natural surfaces are rarely totally impervious, so in the presence of moisture, some of the surplus radiant energy may be converted to latent heat. On the other hand, in the event of precipitation, natural surfaces may absorb much of the additional water, so that the excess moisture is not available at the surface; impervious urban materials, on the other hand, remain wet, and considerable moisture may be evaporated within a short time, increasing the latent heat content of the air and restricting increase in its temperature. In terms of climatic response, there are thus two surface types of great importance: first, impervious surfaces that can cover the full moisture range from 'wet' (after rain) to 'dry' in a very short period, and second, pervious natural surfaces that can cover a similar range, but over more extended periods and with a much slower response.

Urban environments may vary from inner-city surroundings consisting almost entirely of masonry, concrete, asphalt and glass, to suburban developments with dense vegetation and well-irrigated lawns. The former may contribute to a very dry system with very little latent heat, while the latter create more humid microclimates that are dominated by the effects of evapotranspiration. In the extreme case of large bodies of water, such as a sea or lake, mixing of the water reduces diurnal temperature fluctuations near the surface,

while high atmospheric humidity restricts evaporation, so both sensible and latent heat fluxes may be small (Akagawa et al., 1995).

Grimmond and Oke (1995) compared the heat fluxes from summertime observations in the suburbs of four North American cities. The authors report that where precipitation is limited and irrigation is practiced, the Bowen ratio[3] β was typically about 1.5, compared with a value of about 0.8-1.0 for cities with frequent summertime precipitation. The daytime Bowen ratio was also affected strongly by the extent of the irrigated area in the cities, there being a clear inverse relationship between β and the irrigated area. Considerable variability in the size of the fluxes was found on a day-to-day basis, but all cities exhibited peak values for Q_E of about 150-200 W m^{-2}, on average, while the magnitude of mean Q_H (sensible heat flux) was about 300 W m^{-2} in Tucson and about 200-225 W m^{-2} in the other cities studied.

A similar study carried out in a suburban location in Christchurch, New Zealand reported similar values for the Bowen ratio in summer, while storage flux remained substantially smaller than total turbulent fluxes (Spronken-Smith, 1998). However the same study also found that in winter, not only is the net radiation Q^* smaller, but also much of the solar energy is absorbed in the soil. Turbulent fluxes (the sum of sensible and latent heat) were found to be quite small, accounting for less than 20% of net radiation, and in some cases exhibiting negative values. Concurrently, net storage accounted for anywhere between 74-98% of mean daily net radiation.

Grimmond and Oke (2002) proposed the following expressions for calculation of the sensible and latent heat fluxes near the surface:

$$Q_H = \frac{(1-\alpha)+(\gamma/s)}{1+(\gamma/s)}(Q*-\Delta Q_s)-\beta \qquad (2.30.)$$

$$Q_E = \frac{\alpha}{1+(\gamma/s)}(Q*-\Delta Q_s)+\beta \qquad (2.31.)$$

where s is the slope of the saturation vapour pressure-versus-temperature curve; γ is the psychrometric constant; and α and β are empirical parameters. α depends on the soil moisture status, and accounts for the strong correlation of Q_H and Q_E with Q^*-ΔQ_S, whereas β accounts for the uncorrelated portion. Equation 2.30 is essentially the same as the Priestley-Taylor equation (equation 2.26), which was originally proposed to calculate evaporation in the presence of unlimited moisture (over large bodies of water or saturated soil). Extension to non-saturated areas is enabled by the addition of the empirical factor β and by selecting appropriate values for α. It is much simpler than Brutsaert and Strickler's equation (equation 3.27), but its accuracy depends on whether the values of α and β are appropriate for the conditions.

[3] The Bowen ratio (β) is the ratio between sensible heat flux and latent heat flux in a given location. When there is a shortage of water and evapotranspiration is limited, β>1, reaching values of 10 or more in desert conditions. The Bowen ratio for temperate areas is typically 0.4-0.8.

Previous work by Hanna and Chang (1992) and Beljaars and Holtslag (1989, 1991) suggested that the value of β is independent of local conditions, whereas α increases from nearly zero in hyper-arid conditions to a maximum of about 1.2-1.4.

Table 2.5: Values of the α and β parameters *(Hanna & Chang, 1992)*.

	α	β (Wm^{-2})
Dry desert with no rain for months	0.0-0.2	20
Arid rural area	0.2-0.4	20
Crops and field, midsummer during periods when rain has not fallen for several days	0.4-0.6	20
Urban environments, some parks	0.5-1.0	20
Crops, fields or forests with sufficient soil moisture	0.8-1.2	20
Large lakes or ocean with land more than 10km distant	1.2-1.4	20

More recently, Grimmond and Oke (2002) tested the above values of the α and β parameters against data from well-documented observations in several North American cities, and substantial variations were found. The value of α ranged from 0.19 in dry Mexico City to 0.71 in cool and humid Chicago, with an average value of 0.45. β ranged from –0.3 in Mexico City to 8.4 in Tucson, averaging only 2.8 W m^{-2} - substantially less than previously reported.

Finally, it is worth noting that the effect of a given input of anthropogenic heat on urban air temperature also depends on the amount of moisture present (Torrance and Shum, 1976). The presence of moisture, regardless of source (atmospheric, vegetation etc.) results in a larger latent heat component, at the expense of sensible heat.

2.5 Wind and turbulence

The planetary boundary layer

When a viscous fluid such as air flows over a surface, the surface exerts frictional drag on it, affecting the properties of the flow. The portion of the fluid in which the effects of the solid surface are felt is known as the *boundary layer*. Davenport (1965) found that wind speed in the earth's atmospheric boundary layer (also known as the planetary boundary layer, or PBL) increased with height above the surface, and that the mean wind speed $\overline{u}$ at any height z above the surface could be calculated by a simple power law:

$$\overline{u}_z = V_G \left(\frac{z}{z_G}\right)^{\alpha} \qquad (2.32.)$$

where V_G is the geostrophic wind, z_G the height at which the effects of the earth's surface on the geostrophic wind were no longer felt (i.e. the depth of the PBL), and α the exponent of the power law. The value of α

depends both on the surface roughness and atmospheric stability, and may range from about 0.1 for smooth water to about 0.4 for well-developed urban surfaces (Arya, 1988). Empirical evidence led to the conclusion that the rough urban surface not only changed the shape of the velocity profile, but also increased the height of the boundary layer.

Table 2.6: The vertical wind profile for different terrain types *(Davenport, 1965)*.

While Davenport's empirical findings have been quoted very often, physical analysis leads to the conclusion that in a neutrally stable atmosphere, the wind speed u_Z at height z above the surface depends not only on height but also on the surface drag and on the density of the fluid (Arya, 1988). The velocity scale is given by a quantity known as the *friction velocity* u^*, which is equal to $(\tau_0/\rho)^{1/2}$, by definition, and where τ_0 is the surface drag and ρ fluid density. The wind speed at height z is then given by a logarithmic relation (rather than a power law):

$$u_z = \frac{u_*}{\kappa}\ln(\frac{z}{z_0}) \qquad (2.33.)$$

where u_* is the friction velocity, κ is the von Karman constant (0.40), and z_0 is a constant termed the *roughness length* such that $u=0$ when $z=z_0$.

The roughness of a surface may be visualized as a series of individual elements protruding above a smooth plane. Each of these elements creates a disturbance to the flow. The distance between them determines whether these disturbances are wholly separate in space, or whether they are overlaid, resulting in complex flow patterns. When the roughness elements on the surface are sufficiently dense, a skimming flow patterns develops. Evaluation of z_0 in such cases cannot refer to the ground surface, since most of the momentum transfer occurs near the top of the elements. It is useful to define a *zero-plane displacement* z_d so that the roughness length of the surface is measured from an imaginary plane above the ground, and the logarithmic profile equation is then modified accordingly:

$$u_z = \frac{u_*}{\kappa}\ln(\frac{z-z_d}{z_0}) \qquad (2.34.)$$

The logarithmic wind profile described above is valid in the absence of thermal buoyancy, i.e. under conditions when a packet of air will have neither a tendency to rise or to subside. A neutrally stable atmosphere is not the general rule, however: The atmosphere is often either stable or unstable.

The effect of stability on the evolution of eddies and hence on the vertical profile of wind is shown in schematic form in Figure 2.3 (after Thom, 1975)

NOTE:
This figure is included on page 31
of the print copy of the thesis held in
the University of Adelaide Library.

Figure 2.3: Wind speed profiles and simplified eddy structures characteristic of the three basic stability states in airflow near the ground *(Thom, 1975).*

Atmospheric stability is generally described by one of the following parameters (Monteith and Unsworth, 1990):

a. The Richardson number (Ri) is the ratio of buoyancy forces to inertial forces in the air, and may be calculated from gradients of temperature and wind speed:

$$Ri = \frac{g}{T} \cdot \frac{\left(\Delta \overline{T} / \Delta z\right)}{\left(\Delta \overline{u} / \Delta z\right)^2} \qquad (2.35.)$$

where g is the acceleration due to gravity, $\overline{T}$ is the mean temperature in the layer Δz and $\overline{u}$ is the mean horizontal wind speed in the layer. When -0.01<Ri<+0.01 convection is considered to be 'fully forced'. As Ri approaches +0.2, turbulent exchange is inhibited, and there is no convection. When Ri is less than –1, free convection dominates.

b. The Obukhov length [4] is a function of fluxes of heat and momentum. It corresponds to the height at which the shear and buoyant production of turbulent kinetic energy are equal. It is negative under unstable conditions, infinite at neutral stability and positive in a stable atmosphere.

$$L = -\frac{\rho c_p T u_*^{\ 3}}{kgQ_H} \qquad (2.36.)$$

where ρ, c_p and T are the density of air, its specific heat and its absolute temperature, u_* is the friction velocity, k is the von Karman constant, g is the acceleration due to gravity and Q_H the turbulent sensible heat flux.

If the atmosphere is not neutrally stable, equation 2.33 above must be modified to account for buoyancy effects, as follows:

$$u_z = \frac{u_*}{\kappa}\left[\ln\left(\frac{z - z_d}{z_0}\right) - \Psi_m\left(\frac{z}{L}\right)\right] \qquad (2.37.)$$

where Ψ_m is a stability function and L is the Obukhov length.

The urban boundary layer (UBL)

When regional winds blow over a city, the planetary boundary layer (PBL) is modified as a result of contact with the urban surface, which is rougher than most natural surfaces. The urban surface is often extremely varied in character: Its patchy and heterogeneous nature means that turbulence characteristics (including fluxes) measured at a certain height over a complex urban landscape may not be in equilibrium with the surface below, but may instead reflect the characteristics of the surface upwind (Arnfield, 2003). The size and location of the source area depend on the wind speed and direction, surface roughness and atmospheric stability (Schmid and Oke, 1990).

[4] The Monin-Obukhov similarity theory (MOST) provides the conceptual framework for describing the mean and turbulence structure of the stratified surface layer (the part of the atmosphere which is fully adapted to the surface, but is above the height affected by individual roughness elements). This theory proposes that in a horizontally homogeneous layer the mean flow and turbulence characteristics depend only on four independent variables: the height above the surface, z; the friction velocity, u_*, the surface kinematic heat flux, $H_0/\rho c_p$; and the buoyancy variable g/T_0. The theory requires several simplifying assumptions, as follows: The flow is horizontally homogeneous and quasi-stationary; the turbulent fluxes of momentum and heat are constant with height; molecular exchanges are insignificant in comparison with turbulent exchanges; Coriolis effects may be ignored; and the influence of surface roughness, boundary layer height and geostrophic winds is fully accounted for through u_*. Because independent variables in the M-O similarity theory involve three fundamental dimensions (length, time and temperature), according to Buckingham's theorem one can formulate only one independent dimensionless combination of them. The combination chosen by M-O is the buoyancy parameter ξ, so that $\xi = z/L$, where L is the Obukhov length. It is worth noting that recent experimental evidence suggests that in very stable conditions, the assumption of height-independent momentum flux may not be always be justified ((Pahlow *et al.*, 2001). Furthermore, Feigenwinter *et al.* (1999) note that the assumption that turbulent fluxes are constant with height is not justified over rough urban terrain, except at very small spatial scale.

The lower portion of the atmosphere over a city may be divided into several sub-layers (Figure 2.3):

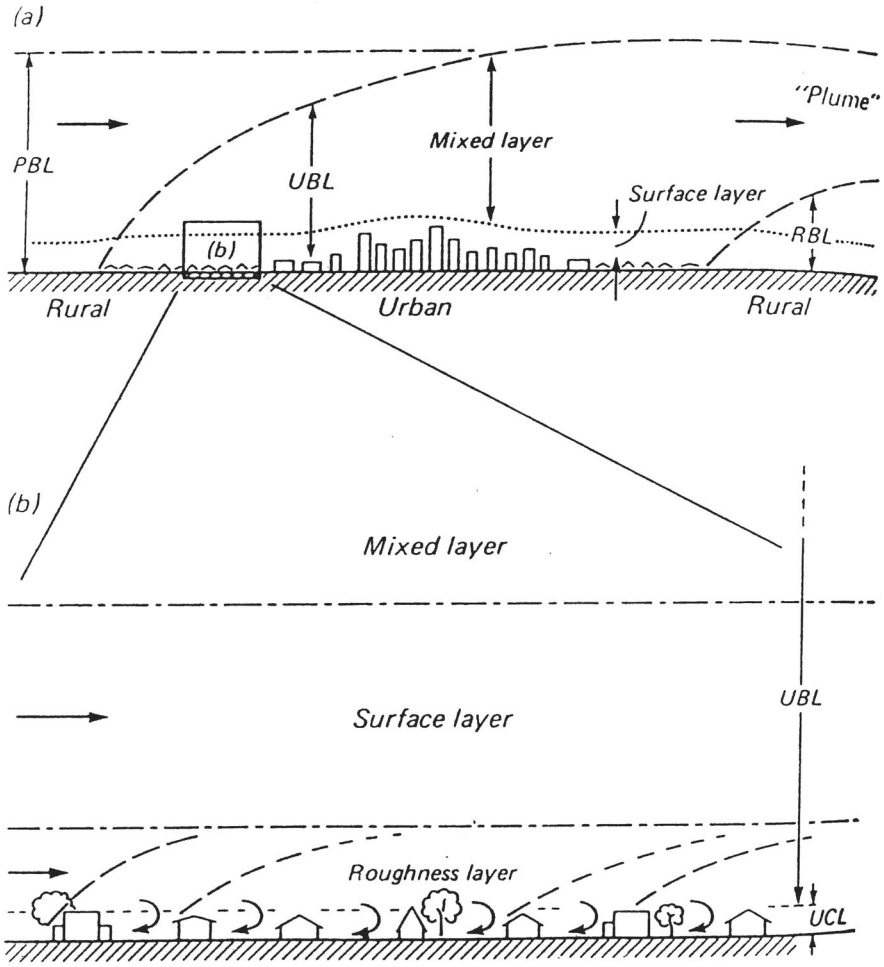

Figure 2.4: Conceptual arrangement of boundary layer structure over city: (a) at the meso-scale (~10km); (b) at the local scale (10^{-1}km). *(Schmid et al, 1990)*

- The *urban canopy layer (UCL)*, comprising the air between buildings, approximately up to roof top height.
- The *roughness sub-layer* (also referred to as the *turbulent wake layer* or the *transition layer*), in which flow consists of interacting wakes and plumes of heat, humidity and pollutants introduced by individual roughness elements. The heterogenous nature of most urban surfaces, comprising rigid buildings of different heights, vegetation and open spaces of various dimensions often result in the development of a roughness sub-layer whose depth may be several times the average building height.
- The *inertial sub-layer* (also known as the *constant-flux layer*) is found above the roughness sub-layer. In it, the blending effect of turbulent mixing erases the significance of individual roughness elements. The inertial sub-layer is thus a layer in which turbulent fluxes are constant with height, permitting measurement of energy-balance fluxes on a landscape scale. Under adiabatic conditions, height

above the effective surface is the only controlling length scale in this layer, and the semi-logarithmic profile laws are obeyed (Roth *et al*., 1989).

- The *mixed layer*, which lies above the inertial sub-layer, comprises the bulk of the urban boundary layer. Within this layer the atmosphere is influenced by the presence of the urban surface, but is not fully adapted to it. In other words, the impact of the regional (rural) wind is still felt in it. The height of the mixed layer varies according to atmospheric stability and the magnitude of the urban effects, and differs substantially from the rural PBL, especially at night (Baklanov, 2001). A good estimate of the upper limit of the mixed layer, above which the presence of the city is not felt at all, is probably about 5-10 times the height of the inertial sub-layer (Wieringa, 1993).

The roughness sublayer and the inertial sublayer form what is sometimes referred to as the *surface layer*, though this term sometimes refers to the inertial sublayer only.

Surface roughness length and zero-plane displacement in urban environments

There are two different methods to describe the roughness of the surface: The *roughness length* z_0 and the *drag coefficient* $C_{D(z)}$. The size of the drag coefficient depends on the choice of reference height, so z_0, which is independent of height (over a homogeneous terrain), is often preferred as a basic descriptive parameter of the surface roughness.

There have been numerous attempts to estimate the size of the roughness length of various terrain types based on measurements of wind speed at several heights above the surface. Lettau (1969) proposed the following simple relationship:

$$z_0 = \frac{0.5 h^* s}{S} \qquad (2.38.)$$

where h^* is the average height of the roughness elements, s is the silhouette area of the average obstacle and S is the specific lot area of the obstacle. (S is defined so that if n is the number of obstacles in a given lot and A is the area of this lot, then $S=A/n$.) The numerical factor 0.5 corresponds to an average coefficient of drag. Lettau's formulation was limited to a homogeneous surface, but its validity has recently been extended to moderately inhomogeneous situations as well (Petersen, 1997).

Wieringa (1993) presented an exhaustive survey of quantitative studies of the roughness length, and summarised his findings in a table, presented here in partial form (Table 2.7). Wieringa also pointed out, however, that since the values shown in the table were measured over homogeneous surfaces, the roughness length of heterogeneous terrain characterised by wake-interference flow would be significantly higher.

Table 2.7: Typical roughness length of homogeneous surfaces *(Wieringa 1993)*

Surface type	Roughness length (m)
Concrete, flat desert	0.0002-0.0005
Fallow ground	0.001-0.004
Short grass	0.008-0.03
Continuous bushland	0.35-0.45
Mature pine forest	0.8-1.6
Tropical forest	1.7-2.3
Dense low buildings (suburb)	0.4-0.7
Regularly built large town	0.7-1.5

Bottema (1997) proposed analytical expressions for estimating the roughness length and displacement height of regular building groups, which were validated against an exhaustive survey of data reported in the literature, yet the author himself found that it was very difficult to obtain reliable experimental values of z_0 and z_d. Evaluation of the zero-plane displacement and the roughness length in urban terrain has proved to be so difficult because of the complexity and heterogeneous nature of the urban surface, and because the properties of the flux source area affect the results (Rooney, 2001). There are two classes of methods to determine these parameters (Grimmond and Oke, 1998a):

- Micro-meteorologic (or anemometric), which use field observations of wind or turbulence to solve for z_0 and z_d in the logarithmic profile equation
- Morphometric methods, which use algorithms relating z_0 and z_d to measures of surface morphology.

Anemometric studies in real urban locations are expensive and complex, but scale-model studies in wind tunnels cannot reproduce a sufficiently long fetch or boundary layer height to be useful. Grimmond *et al.* (1998) surveyed over fifty field studies of the wind structure in cities. The value of many of these, such as the study reported by Kondo and Yamazawa (1986), is compromised by the fact that they failed to consider critical aspects of this inherent complexity, most commonly the magnitude of the zero plane displacement. Further complicating matters is the fact that in many urban sites the sinks for momentum and energy fluxes are not co-located. This is because most momentum exchange is concentrated on the upwind vertical portions of the main roughness elements (buildings and trees) lying above the zero-plane, while heat exchange occurs over all surfaces, with an effective anisotropy controlled by solar angles (Grimmond *et al*., 1998). Yersel and Goble (1986) noted that large variations in urban roughness lengths, which often show directional dependence, indicate that complex urban areas cannot be assigned a single value of roughness length. Furthermore, the proposition that the zero plane displacement may vary with wind direction, too, is supported by evidence from a field experiment in Zurich (Rotach, 1994), who found that z_d varied between 10-15 metres, giving ratios of z_d / h of 0.5-0.88 (where 'h' is average local building height).

While morphometric methods fail to simulate the full heterogeneity of size, shape, spacing and orientation of buildings, an overview of the definitions used may nonetheless be valuable (Grimmond and Oke, 1999a).

- Plan area index: $\lambda_P = A_p/A_t$, where A_p is the plan area of the roughness elements and A_t is the total area
- Frontal area index: $\lambda_F = \overline{L}_y \overline{z}_H / \overline{D}_x \overline{D}_y$, where $\overline{L}_y$ is the mean breadth of the roughness elements perpendicular to the wind direction, $\overline{Z}_H$ is their mean height and $\overline{D}_x$ and $\overline{D}_y$ the average spacing between element centroids in the along-wind and crosswind directions, respectively.

NOTE:
This figure is included on page 36 of the print copy of the thesis held in the University of Adelaide Library.

Figure 2.5: Definition of surface dimensions used in morphometric analysis *(Grimmond and Oke, 1999).*

None of the models proposed so far has been able to explain more than 24% of the variance in the measured data. However, the conceptual framework proposed by Grimmond and Oke (1999a) is nonetheless the best currently available, and may be summarized in the following figure:

NOTE:
This figure is included on page 36 of the print copy of the thesis held in the University of Adelaide Library.

Figure 2.6: Conceptual representation of the relation between height-normalized values of zero-plane displacement (z_d/z_H) and roughness length (z_0/z_H) and the packing density of roughness elements, (a) using λ_P and (b) using λ_F *(Grimmond and Oke, 1999).*

The following table summarises first-order estimates of the aerodynamic parameters of urban areas proposed by these authors:

Table 2.8: Typical roughness properties of homogeneous zones in urban areas *(Grimmond and Oke, 1998a)*.

NOTE:
This table is included on page 37
of the print copy of the thesis held in
the University of Adelaide Library.

Grimmond and Oke (1998a) also suggest that a rough correlation between building height and the roughness length is z_0 / z_H ~ 0.1 in most urban situations, and that the relation between zero-plane displacement and building height is z_d / z_H ~ 0.5 for low density sites, and 0.6 and 0.7 for medium and high-density sites, respectively.

Recent experimental work based on scintillometers to measure atmospheric fluxes over a large source area suggests that the magnitude of the zero-plane displacement may vary with changes in atmospheric stability (Kanda *et al.*, 2002): Unstable conditions result in larger fluxes, and hence stronger vertical flows, leading to greater mixing of the air in the canopy layer and to smaller values of z_d.

Urban-scale wind

Lowry (1967) claimed that in near-calm or weak-wind and clear-sky conditions, urban-scale thermal flows might be more dominant than regional winds. A thermally induced circulation is imposed on any weak background flow that is directed radially inward towards the city centre at lower levels and outward from the city centre at higher levels. This wind pattern was explained by differences in surface temperature during the morning, when horizontal surfaces reflect much of the incoming radiation from the sun, which is still low in the sky, whereas vertical wall surfaces in the city absorb most of it. When the sun has a higher elevation, near the middle of the day, differences in surface temperature are much smaller, and this flow pattern weakens, only to be reinforced again in the late afternoon when solar elevation is low. This circulation pattern was claimed to extend up to the base of the lowest inversion during the daytime. Support for Lowry's hypothesis may be found in the results of a simulation of meso-scale meteorological conditions using a modified CSU (Colorodo State University) model, which predict the development of a nocturnal convergence zone near the centre of a city as a result of the urban heat island (Khan and Simpson, 2001).

Recent empirical evidence (Thorsson and Eliasson, 2003) suggests that while an intra-urban thermal breeze (IUTB) is possible, it occurs only at night (not in the daytime), and only in very specific meteorological

conditions: if the urban heat island is strong, there is a strong ground based inversion and the meso-scale wind is very weak. It was found that under such conditions, a decoupling of the lower layer of the atmosphere occurred: a surface flow of about 0.3 m s^{-1} was measured towards the city centre, with a return flow of about the same magnitude found at rooftop level.

Haeger-Eugensson and Holmer (1999) suggested that when the urban heat island generates a thermal breeze, which they referred to as 'urban heat island circulation' (UHIC), the resulting advection may act as a self-regulating mechanism that reduces the urban-rural temperature difference. In a study carried out in Goteborg, Sweden, they found that in the presence of a thermal inversion, when the depth of the mixing layer was only 40-60 metres, advection of cool rural air into the city was about 9 +/-4 W m^{-2}, and resulted in a reduction of urban air temperature by about 0.3 K. They proposed that a larger urban-rural temperature difference would result in a stronger flow, which would in turn tend to erode the existing temperature differential.

A variant of the IUTB may occur in the presence of a fairly large park (~1 km^2 in area) surrounded by built-up areas. In stable weather conditions with weak regional winds a *park cool island* ($\Delta T_{u\text{-}p}$>0) is likely to occur, which may induce a local-scale thermal flow sometimes referred to as a *park breeze* (Eliasson and Upmanis, 2000). Air tends to subside over the relatively cool park, and a local airflow of up to 0.5 m s^{-1} is created outwards towards the built-up surroundings in all directions. Such flows are perforce limited in extent, and may be felt less than 250 metres from the park border. They are best developed between two and six hours after sunset.

The extent of urban heat island advection to nearby rural sites was monitored by Brandsma et al. (2003), using temperature data and detailed wind records from several meteorological stations. Heat from neighbouring towns caused a temperature increase of about 0.1 ^oC in an adjacent rural station located in a so-called transition zone. No contribution was detected from much larger but more distant cities.

Wind in the urban canopy layer

While wind in the urban canopy layer is driven to a great extent by meso-scale forces, the surface friction caused by buildings dominates the development of the boundary layer in this region (Goliger and Milford, 1991). Failure to recognize this fact has often led to the application of the semi-logarithmic profile of wind speed in the planetary boundary outside its range of validity, by extrapolating it down to $z=d+z_0$ (the theoretical zero-velocity level). Macdonald (2000) noted that in reality, mean wind speed in the canopy layer could be predicted by an exponential curve that would match the semi-logarithmic profile at the wake diffusion height z_w, giving a continuous profile.

According to MacDonald, the mean horizontal component of the wind U at height z above the ground is

$$U_z = U_H^{(a(z/H-1))} \qquad (2.39.)$$

where U_H is the mean wind speed at the height of the top of the buildings H, and a is an attenuation constant. The value of a is proportional to the ratio of the mean sectional drag coefficient of individual buildings C'_D and the total drag coefficient for the array C_{DH}:

$$a = \frac{C'_D}{2C_{DH}} \tag{2.40.}$$

Experimental data from wind tunnel experiments suggests that an approximate value for the attenuation coefficient is a =9.6λ_F, where λ_F is the frontal area index. The same wind tunnel studies also confirmed the exponential form of the vertical profile of wind in the urban canopy, for simplified urban configurations.

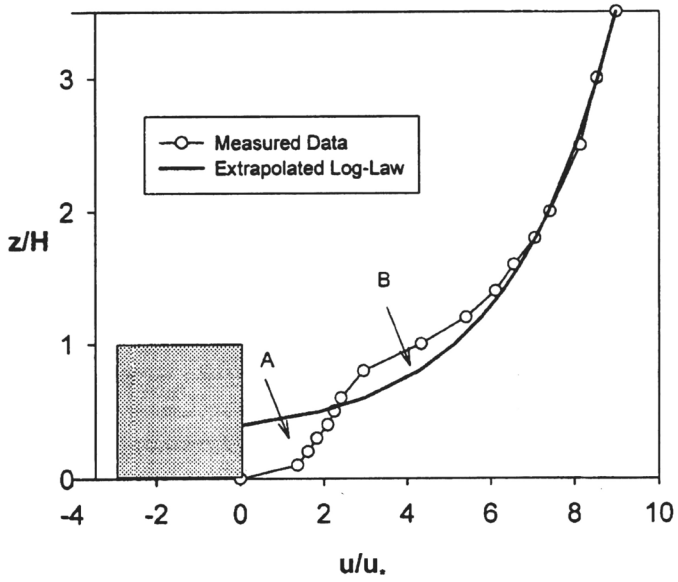

Figure 2.7: Comparison of the extrapolated log profile with measured data from a wind tunnel experiment, illustrating the actual vertical profile of the mean wind speed in an urban area *(MacDonald, 2000).*

The profiles giving the mean wind speed in the boundary layer are not sufficient to describe the actual flow conditions at any given point. The complexity of the urban form means that in addition to affecting wind speed, buildings also affect the structure of the eddies and the direction of flow. Oke (1988a) identified three flow patterns in urban areas, on the basis of a two-dimensional representation of the typical street section (meaning buildings are much longer than they are tall):

- *Isolated roughness flow* occurs when H/W<0.3:
- *Wake interference flow* occurs when 0.3<H/W<0.7
- *Skimming flow* occurs when H/W>0.7

Oke's classification has been confirmed by numerical modelling (Hunter et al., 1990-91). When the approach wind is perpendicular to the street canyon axis, the transition between skimming flow to wake interference was found to occur at aspect ratios of about 0.7-0.75, irrespective of canyon length. The change from a wake

interference pattern to isolated roughness flow, though, is affected by canyon length in addition to the aspect ratio, and occurs at H/W~0.4 for 'cubical canyons (i.e. square courtyards), and at H/W~0.2 for long canyons (L/H>5). Evidence from a field study (Johnson and Hunter, 1999) suggests that skimming flow and the associated in-canyon vortex may be found in canyons with an aspect ratio as low as 0.4, however.

Figure 2.8: Flow regimes associated with different urban geometries *(Oke, 1987).*

The above classification is of necessity a simplification. Urban areas are not two-dimensional, and aerodynamic form could equally be represented by the frontal area density λ_F. Macdonald (2000), for instance, suggests that skimming flow develops when λ_F=0.2, at which point z_0 begins to decrease.

Measurements of wind speed and direction in a fine spatial matrix (Yamartino and Wiegand, 1986) indicated that canyon parallel and transverse flows are largely decoupled from one another. They confirmed the Hotchkiss and Harlow (1973) model that when air flows above a two-dimensional rectangular notch of depth H and width B (in effect – an urban canyon), a vortex is formed. The transverse (horizontal) component of the flow (u) and the vertical component (w) are then given by the following expressions:

$$u = u_0(1-\beta)^{-1}\left[\gamma(1+ky) - \beta(1-ky)/\gamma\right]\sin(kx) \qquad (2.41.)$$

$$w = -u_0 ky(1-\beta)^{-1}[\gamma - \beta/\gamma]\cos(kx) \qquad (2.42.)$$

where $k=\pi/B$: $\beta=exp(-2kH)$; $\gamma=exp(ky)$; $y=z-H$; and u_0 is the transverse wind speed above the canyon (and at the point $x=B/2$, $z=H$).

The transverse flow, which is independent of the along-canyon longitudinal flow, has a simple logarithmic profile:

$$v(z) = v_r \frac{\log\left[\frac{z + z_0}{z_0}\right]}{\log\left[\frac{z_r + z_0}{z_0}\right]} \qquad (2.43.)$$

where v_r is the along-canyon component of the wind speed at reference height r above the canyon and z_0 is the roughness length. (This formulation assumes neutral atmospheric stability and height-independent shearing stress.) Yamartino and Wiegand (1986) also note, however, that z_0 has different values according to different angles of the approach flow with respect to the longitudinal axis of the street.

Several researchers have proposed simplified relationships between the above-canyon flow and mean canyon wind speed. Nakamura and Oke (1988) suggested that for canyons with an aspect ratio of approximately unity, the along-canyon wind speed near the surface is approximately 2/3 of its speed above the canyon roof. Swaid (1993b) commented that since there were three distinct flow regimes corresponding to different canyon aspect ratios, it was reasonable to assume that the ratio between the above-canyon wind and the along-canyon flow near the floor would not be constant. Scale-model measurements in the open air confirmed that the wind diminution factor (defined as the ratio between mean canyon wind speed and ambient wind speed) changed only moderately among canyons belonging to the same airflow category, but changed considerably between canyons characterised by different flow regimes. For example, it increases from 0.51 to 0.59 upon changing from an aspect ratio of 2 to 1 (both characterized by skimming flow), but increases from 0.59 to 0.81 upon changing from H/W of 1 to 2/3 (the latter having a wake interference flow pattern).

The Hotchkiss and Harlow (1973) model is also supported by measurements carried out in an urban canyon in Chicago (DePaul and Sheih, 1986). Using helium balloons, the researchers were able to visualize the vortex formed when ambient wind direction was nearly perpendicular to the street axis (giving an essentially two-dimensional pattern). The vortex became apparent only when rooftop velocity exceeded about 2 m s^{-1}, and velocities computed from the trajectories of the balloons corresponded to model predictions. The observations also confirmed that the vortex did not project above the canyon top - a finding that has important implications for studies of pollutant dispersal, as well as for turbulent diffusion of sensible heat. Finally, it was found that vehicular traffic created substantial turbulence up to a height of about 7 metres above the road surface.

Numerical models (Baik and Kim, 1999; Jeong and Andrews, 2002) as well as scale-model simulations (Baik *et al*., 2000) show that when skimming flow is present, the aspect ratio of the canyon determines the number and strength of the vortices formed in the street. For H/W equalling approximately unity, a single vortex forms, with its centre a little downwind relative to the canyon centre. Deeper canyons are characterised by two counter-rotating vortices. The vertical velocity vector of the primary vortex is independent of the canyon aspect ratio. The downward flow near the downwind wall of the canyon is stronger than the upward flow in

the lee of the windward wall: Johnson and Hunter (1999) suggested that the ratio of these flows is $|w_2|=0.4|w_3|$, where w_2 is the updraft velocity and w_3 the downdraft velocity.

The conventional view of persistent recirculation within the street, in the form of vortices with small-scale turbulent fluctuations about the mean flow, is consistent with some recent field studies (Santamouris *et al*., 1999). However, what has come to be regarded as the orthodox view has recently come under scrutiny. Louka *et al.* (2000) found in a field experiment that while the predicted vortex formed, it was much weaker than the unsteady turbulent fluctuations. According to this view, fluctuations in the position of a shear layer formed by the upstream roof of the street canyon are responsible for the unsteady circulation within the street, and also for the main mechanism of transporting air (and pollutants) from street level into the roughness layer above the roofs. These results confirm earlier findings (Arnfield and Mills, 1994a), which also failed to detect a consistent vortex in wind conditions where one was predicted. The explanation provided at the time was that there was nonetheless evidence for a regular vortex superimposed on otherwise fluctuating, irregular turbulent flow. The same study also found evidence for a consistent mean vertical velocity at the canyon top that was directed *upwards*, indicating a tendency for a decelerating along-canyon wind caused by friction with canyon walls.

A possible explanation for the failure of some field studies to detect clear evidence for a vortex in urban canyon flow is that most models fail to account for thermal effects of differential solar heating of some canyon surfaces. Kim and Baik (1998) simulated the effects of heating individual surfaces, and found substantial thermal flows affecting the mechanical, wind-induced patterns. Sini *et al.* (1996) proposed that if the downwind wall is exposed to direct solar radiation and is substantially warmer than other canyon surfaces, an upwards thermal flow may form near the wall surface. This flow tends to counteract the downwards advective flow, and may lead to the creation of two counter-rotating vortices normally associated with deeper canyons. The formation of a multi-vortex pattern reduces vertical exchanges, primarily of pollutants but also of heat.

Atmospheric stability also affects flow in urban street canyons (Uehara *et al*., 2000). A wind tunnel study showed that cavity eddies that arose in the canyon tended to be weak when the atmosphere was stable and strong when it was unstable. Furthermore, stable atmospheric conditions led to a positive feedback effect in which the downward flow into the street canyon weakened due to buoyancy, which facilitated the formation of more highly stable stratification. As a result, when stability exceeded a certain threshold (in the range Ri_B = 0.4-0.8) the wind speed in the canyon dropped nearly to zero.

Wind in the roughness sub-layer

The roughness sub-layer is the portion of the urban atmosphere immediately above the canopy layer. The processes taking place in this layer have a great effect on the city climate, primarily with respect to the turbulent dissipation of sensible heat and the diffusion of atmospheric pollutants generated at street level.

Rafailidis (1997) estimated that the height of this layer was equal to approximately three times the overall building height. A series of wind tunnel experiments indicated that the effect of flat-roofed buildings on flow

above roof level was quite small compared with the effect of pitched roofs. In fact, the vertical profile of wind above a model city with flat roofs was almost the same as that over a flat plate, for building densities represented by a canyon aspect ratio equal to unity (or more), indicating that skimming flow was fully developed, and the zero-plane displacement d was nearly equal to building height. Rafailidis noted that in such closely packed urban configurations, vertical velocity and horizontal turbulence were relatively weak at roof height: the aeration of the street-canyon is due mainly to vertical turbulence. In contrast, pitched roofs resulted in much greater turbulence above roof level, in both the longitudinal and vertical components of the flow. Pitched roofs therefore promote a much stronger coupling of the canopy layer with the air above roof level. This has important implications for both the thermal balance and for the dissipation of pollutants.

Flux-profile relationships

Meteorological models use flux-profile relationships to calculate vertical fluxes of heat, moisture and momentum as functions of the temperature, humidity and wind speed gradients. The Monin-Obukhov similarity theory predicts that in the horizontally homogeneous atmospheric surface layer, these flux-profile relationships are uniform functions of z_1/L, where z_1 is the reference height and L is the Obukhov length (see definition above). These functions have been determined by experiment for unobstructed surfaces. However, the functions are highly non-linear, and an iteration procedure is required to solve for u*, the friction velocity, and θ*, a temperature scale indicating the surface buoyancy flux.

Louis (1979) derived an explicit expression for the stability functions for a given roughness length of momentum z_{0m}, which depends on the bulk Richardson number Ri_B

$$Ri_B = \frac{z_1 g(\theta_1 - \theta_0)}{TU_1^2} \qquad (2.44.)$$

where θ_1-θ_0 is the temperature difference between the reference height and the level $z=z_{0m}$, U_1 is the wind speed at the reference height and T the reference temperature. Louis assumed that the roughness lengths for heat z_{oh} and for momentum z_{0m} are identical. However, later studies indicate that this is generally not the case, and that they may in fact differ by an order of magnitude (Garratt, 1992). A number of alternative parameterisations have since been proposed that incorporate different values for the roughness lengths of heat and momentum, such as Mascart *et al.* (1995). However, they all incorporate the Richardson bulk number as a measure of the effect of atmospheric stability. A different approach, using the Monin-Obukhov length L as in indicator of stability was proposed by Van den Hurk and Holtslag (1997). In their model, dimensionless transfer coefficients for momentum (C_M) and heat (C_H) are parameterised by means of the Businger *et al.* (1971) stability functions of the MOST framework. The difference between z_{oh} and z_{om} is accounted for explicitly by means of a correction term.

All of the above models share two serious shortcomings: a) There is mounting evidence that the Monin-Obukhov theory may not be applicable to many urban environments, because the atmospheric surface layer

above cities is not horizontally homogeneous, and b) The empirical relationships obtained for flat terrain by Businger *et al.* in the Kansas Plains experiment are unlikely to be sufficiently accurate to represent conditions above a rough urban surface.

Scalar fluxes from urban street canyons

Flux-profile relations are useful tools for modelling the vertical profiles of a quantity such as heat or momentum where the horizontal dimensions of the area being analysed are relatively large, and conditions within the area are homogeneous. However, airflow within urban canyons is complex and the assumption of homogeneity is not justified, so accurate modelling of fluxes within them requires a detailed description of individual surfaces, as well as the of the interface between different flow regions. This in turn requires a methodology for linking the fluxes among the component regions in a coherent and consistent framework. Such a methodology has been proposed that is based on a resistance network, in which the transfer of a scalar between adjacent nodes is governed by the difference in concentration and a resistance to flow (Barlow *et al*., 2004; Harman *et al*., 2004). An advantage of this methodology is that since resistances, unlike transfer coefficients, are additive, transfer of a scalar such as sensible heat between non-adjacent nodes in the network may be modelled. The urban canyon system is treated as a network in which each of the surfaces (walls, road and roof) is represented by a node, as are the air inside the canyon and the air in the roughness layer above it (Figure 2.8).

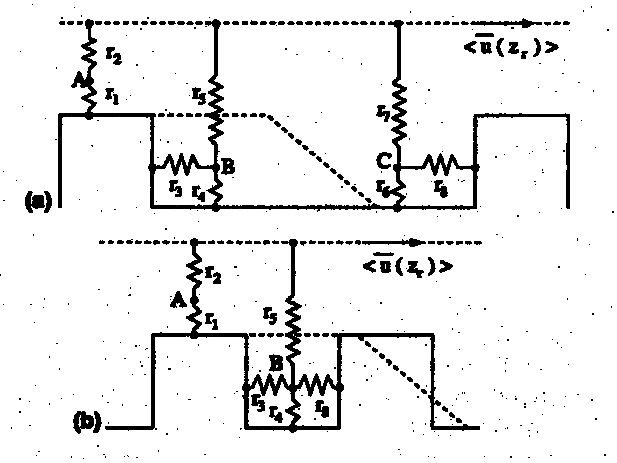

Figure 2.9: The resistance network for (a) a wide canyon, where there are distinct recirculation and ventilation regions, and (b) a narrow canyon, where there is only a recirculation region (Harman *et al.*, 2004).

A resistance is applied to the transfer of energy between each pair of adjacent nodes, the magnitude of which depends on aerodynamic properties of the flow and which is calculated by an appropriate relationship. The model incorporates, in addition to parameters describing roughness lengths of the surfaces and a measure of building height, two empirical parameters that were determined in a wind tunnel experiment and which measured the rate of sublimation of a layer of naphthalene applied on the surfaces of a scale model.

The experiment was, however, carried out in conditions that simulate neutral stability only, so the application of the model to real-life situations is still limited. A further complication is that calculation of the resistance to the transfer of a scalar from a solid surface to the adjacent air requires *a priori* knowledge of the relevant roughness length, which is generally not the same as the roughness length for momentum and may be a function of time-variable environmental conditions, too.

Spatial variability of energy fluxes in urban terrain

The urban surface has often been considered to be homogeneous with respect to energy fluxes; so many early models assumed that in the interest of simplicity, net advection between different parts of the city may be neglected. However, Schmid (1991) found that energy fluxes over a "homogeneous" suburban residential area varied by up to 40% within horizontal scales of only 100-1000 metres. These variations are comparable in magnitude to urban-rural differences. Such horizontal variations of vertical turbulent energy fluxes in the presence of a mean flow must induce advection. This implies that "micro-advection" may have an important effect on the energy balance of urban locations. Spatial variation of net radiant flux was found to be relatively small, while anthropogenic heat varied more substantially, on both spatial and temporal scales. However, the most important differences were found in the partition of sensible and latent heat flux, and in storage heat, resulting from differences between paved and vegetated surfaces, especially if the soil was moist. Changing wind directions imply that the source area for heat advected to a given location may be time-dependent.

The extent and distance of the source area for a given quantity may be modelled using a reverse plume scheme proposed by Schmid and Oke (1990). Grimmond *et al.* (1996) indicated that during the daytime, under unstable atmospheric conditions, the source areas affecting fluxes at a given urban location are most likely contained within an area with a radius of about 500 metres upwind. At night, as the atmosphere becomes neutral or stable, the source areas become narrower and more elongated, and may extend as much as 2000 metres upwind (though distant sources have a much smaller effect than near ones).

2.6 Anthropogenic heat

The release of heat due to combustion of fuels is a heat source for the city not found in uninhabited surroundings. Sailor and Lu (2004) proposed a methodology for estimating anthropogenic heat on the basis of separate analyses of three components,

$$Q_F = Q_V + Q_B + Q_M \tag{2.45.}$$

whereby the total input Q_F is the sum of inputs of vehicles, buildings and (human) metabolism.

Heat from vehicular traffic may be estimated on the basis of detailed hourly traffic counts on major and minor roadways throughout a metropolitan area, which are available to transport engineers in many cities. Traffic patterns in most cities display a pronounced diurnal and weekly pattern, with well-defined rush-hour peaks on weekdays and much lower levels at night and on weekends.

Heat from buildings comprises electricity consumption that powers lighting, air conditioning and equipment, and heating fuels, such as natural gas, which may be used to power space heating in cold climates. Data on electricity consumption are easier to obtain on a detailed scale than information on the use of heating fuels. Modelling the latter is often done on the assumption that overall consumption for a period can be distributed over all buildings in a given area on the basis of floor area, while the rate of use is proportional to the difference between ambient air temperature and some arbitrary fixed interior air temperature.

Heat released from human metabolism depends mainly on population density. Large-scale movements of people commuting to and from work, mostly in downtown locations, affect the spatial distribution of the output of metabolic heat. However, except in extreme cases, this component of anthropogenic heat contributes only 2-3% of the total heat (Sailor and Lu, 2004).

In the absence of a detailed database of heat sources in a city, Elnahas and Williamson (1997) suggest, following Moriyama (1988), that the local anthropogenic flux in a given location may be related to the mean flux for the urban area as a whole through the vegetation ratio at the site (notation adapted):

$$Q_F = (1 - R_g) Q_{F(0)} \tag{2.46.}$$

where $Q_{F(0)}$ is the density of anthropogenic heat released when the vegetation ratio R_g is equal to zero. (The vegetation ratio is the ratio between the vegetated area and the overall area of the site.)

Magnitude

As Table 2.9 shows, the magnitude of anthropogenic heat varies greatly between cities, according to per capita energy use and population density, and depends on the climate (due to the demand for space heating or cooling), the degree and type of industrial activity and the type of urban transport system.

Table 2.9: Average annual anthropogenic heat flux densities *(Oke, 1988b)*.

urban area	year	population density (persons km^{-2}x10^{-3}	per capita energy use (GJ yr^{-1})	Q_F (W m^{-2})	Q* (W m^{-2})	Q_F/Q^*
Manhattan (40°N)	1965	28.8	169	159	93	1.71
Moscow (56°N)	1970	7.3	530	127	42	3.02
Montreal (45°N)	1961	14.1	221	99	52	1.90
Budapest (47°N)	1970	11.5	118	43	46	0.93
Hong Kong (22°N)	1971	37.2	28	33	~110	0.30
Osaka (35°N)	1970-74	14.6	55	26		
Los Angeles (34°N)	1965-70	2.0	331	21	108	0.19
West Berlin (52°N)	1967	9.8	67	21	57	0.37
Vancouver (49°N)	1970	5.4	112	19	57	0.33
Sheffield (53°N)	1952	10.4	58	19	56	0.34
Fairbanks (64°N)	1967-75	0.55	314	6	18	0.33

Sources: Bowling and Benson (1978); Kalma and Necombe (1976); Ojima and Moriyama (1982); Oke (1987); SMIC (1971).

* All data relate to areas within the urbanized limits of the cities, not their surrounding territories.

Oke (1988b) reported average annual values of anthropogenic heat anywhere between 6 W m^{-2} (Fairbanks, Alaska) and 159 W m^{-2} (Manhattan). Ichinose *et al.* (1999), however, in an extremely detailed study, found that anthropogenic heat flux in central Tokyo exceeded 400 W m^{-2} in daytime, with a maximum value of 1590 W m^{-2} in some city blocks in winter. Such great disparity in reported heat fluxes apparently reflects not only real differences between the cities in question, but also differences in calculation methods and definitions.

The method applied by Ichinose *et al.* (1999) is conceptually simple: The total amount of energy consumed in a given urban district was divided by its plan area. In the study of Tokyo, a very fine spatial mesh was used – only 25 metres between adjacent points, and thus required an extremely detailed database. However, the high spatial resolution also created problems, since the presence of as few as one or two high-rise offices or hotels in a grid cell could result in extremely high energy consumption figures for the cell.

From a modelling point of view, this methodology raises several problems:

- Scale of grid cell: In the absence of net advection, the anthropogenic heat flux into a given urban canyon originates from adjacent buildings only. The model should therefore accommodate input of data at an appropriate scale (if available) – and not necessarily city-wide averages.
- Location of heat source: Anthropogenic heat may be allocated uniformly to the whole grid cell at ground level, as is commonly done in meso-scale models. This is a gross simplification, however, because in high-rise buildings, energy flow through the building envelope is distributed along the entire surface area of the building, and much of it will not affect conditions in the urban canyon directly. This is especially true in hot climates, where heat exchangers for air conditioning equipment of multi-storey buildings are often located on the roof. Whereas wall or window-mounted air conditioners dump the excess heat directly onto the street where it contributes to the urban canopy layer heat island, central air conditioning systems in high-rise buildings in effect transport energy from the canopy layer near street level to the roughness sub-layer above the roof, where it is quickly dissipated.
- Mode of heat transfer: Energy may be emitted (or absorbed) in the form of sensible heat, e.g. in heat exchangers of air conditioners, contributing directly to the canopy layer heat island. However, it is also exchanged by radiation, for example from warm building surfaces, and may be in the form of latent heat through vaporisation. Each of these processes must be accounted for in models of the urban environment, according to the level of spatial detail and time step being simulated.
- Correlation between energy consumption and heat flux to the environment: Ichinose *et al.* (1999) assumed that energy consumption is equivalent to anthropogenic heat, since ultimately all consumed energy is transformed into heat. However, the same research found that in many of the buildings studied, as much as 50% of the energy consumed was required to heat water – much of which was later released into the sewage system, and thus had only a minor effect on local air temperature.

An alternative approach to that used by Ichinose *et al.* (1999) is to assess anthropogenic heat by considering heat conduction through building envelopes. If the interior temperature of the building and the thermal properties of its external envelope are known, there is no need to assemble overall energy consumption data (other than inputs due to vehicles and other external sources). This is the approach employed in many of urban canyon models, which are not intended to provide meso-scale data, Mills (1997b) for example.

Spatial variability

The values quoted above are representative values for entire cities, and mask great spatial variability within the metropolitan area. Sailor and Lu (2004), for instance, suggest that the anthropogenic heating contribution in urban cores of U.S. cities may be 5-10 times greater than the magnitudes of city-wide averages reported in their paper.

Older data from Sydney (Kalma, 1974) show an even greater discrepancy, with anthropogenic heat varying between about 1 W m^{-2} in the outlying suburbs of the city to over 25 W m^{-2} in the CBD at 07-09 h on an average July. The actual figures for anthropogenic energy use given above are not representative of current (2004) levels, which are much higher. However, they are still valid as indicators of the extreme disparities found within the Sydney metropolitan area - and of many other cities with a dense urban core and extensive suburbs.

Temporal variability

The mean annual values mask great *temporal* as well as *spatial* variability. Anthropogenic heat emissions parallel levels of human activity, and therefore have daily, weekly and seasonal cycles.

Sailor and Lu (2004) reported in their study of U.S. cities that Chicago, San Francisco and Philadelphia had wintertime anthropogenic heating loads of 70-75 W m^{-2}, averaged over the entire city, compared with only 30-60 W m^{-2} in summer. In each of these cities, heat from vehicles was the dominant source in summer, accounting for 47-62% of the total. In winter, the contribution of heating fuels increased to over 50% in the cold climate cities.

Another important finding of the Sailor and Lu (2004) study was that all U.S. cities surveyed displayed the same typical diurnal pattern, irrespective of season, location or weather: Anthropogenic heat was at a minimum at night, with consumption more than doubling during the daytime, between about 7 a.m. and 4 p.m. Two distinct peaks, reflecting the contribution of rush-hour traffic, were clearly distinguishable in all cities, at about 8 a.m. and 4 p.m.

Previous studies in other countries had similar findings. For instance, the anthropogenic heat flux in central Sydney (in 1970) was estimated to have a daytime maximum of approximately 60 W m^{-2} in January but nearly 80 W m^{-2} in July, with similar night-time minima of about 30 W m^{-2} (Kalma and Newcombe, 1976).

Daily variations were also reported by Ichinose *et al.* (1999), who noted that in winter, office demand peaked at about 9 a.m., then declined slowly throughout the day, while hotels typically had low demand throughout the day and a large demand in the evening, while residential demand had twin peaks at 8 a.m. and at 9 p.m.

A detailed study carried out in Brisbane (Khan and Simpson, 2001) showed, as may be expected, substantial differences between anthropogenic contributions in major urban areas compared with suburban areas. Motor vehicles were found to be the major contributor of energy, responsible for approximately 72% of the anthropogenic heat during the morning rush hour. The daily pattern of overall consumption reflects the predominance of this source in the city centre, varying from a minimum of about 17 W m^{-2} at night, to about 33 W m^{-2} around mid-day, with peaks of about 66 W m^{-2} and 57 W m^{-2} corresponding to the morning and afternoon rush hour periods, respectively. It should be noted, though, that the relatively mild climate of Brisbane results in a modest demand for space conditioning, which in more extreme climates would account for a larger proportion of energy consumed and released to the environment.

Seasonal variations in energy demand reflect changing demand for space conditioning, artificial lighting etc. However, the effect of these absolute changes in the magnitude of the fluxes may be less important than the change in the relative magnitude of the fluxes due to changes in meteorological conditions, such as solar insolation and ambient air temperature. For example, as a proportion of the average daily insolation, artificial heat generation in central Sydney was 17.4% in January, but 48.9% in July, when sunshine was less abundant and energy use higher (Kalma *et al.*, 1972). Likewise, Ichinose *et al.* (1999) noted that in Tokyo, solar radiation was strong in summer and the effect of anthropogenic heat relatively small, but in winter the situation was reversed.

2.7 The effects of vegetation

Vegetation affects conditions in the city in a variety of ways. For instance, several studies found that vegetation dry-precipitates and adsorbs pollutants and by doing so, decreases the mass of airborne gases and particulate matter (Raza et al., 1990-91; Taha et al., 1997). However the following section deals only with energy-related aspects of vegetation in the city.

The effects of vegetation on the energy balance are compound:

1. In a thickly vegetated area, the ground surface is no longer the most appropriate datum for the surface energy balance: Radiative, sensible and latent heat fluxes are spatially variable within the vegetative canopy, and must be dealt with taking into account the following factors:
    a. Reduced penetration of short wave solar radiation to the ground surface.
    b. Interception of long wave (infra red) radiation from the ground surface to the atmosphere.
    c. Reduced wind speed and lessened advection.
    d. Reduced surface run-off of water (after rain events) compared with paved surfaces or bare ground.
2. Energy storage in plants, unlike inanimate surfaces, consists of two separate components:

a. Physical heat storage
b. Bio-chemical energy storage (the result of photosynthesis and CO_2 exchange)

3. Latent heat exchange occurs not only due to condensation or evaporation at the ground surface, but to a large extent due to evapotranspiration from plant leaves.

Urban evapotranspiration rates

Grimmond and Oke (1991) extended previous work to encompass the effects of vegetation on the rate of evapotranspiration in an urban setting. The urban canopy is likened to a true forest, in which building walls represent tree trunks, albeit with a much smaller surface area. The latent heat flux Q_E is calculated using the Monteith version of the Penman equation, modified for urban surroundings

$$Q_E = \frac{s}{s+\gamma} \cdot \frac{(Q^* + Q_F - \Delta Q_s) + (C_a V)/r_a}{(1 + r_s / r_a)} \qquad (2.47.)$$

where s is the slope of the saturation vapour pressure vs. temperature curve (Pa K^{-1}); γ is the psychrometric constant (Pa K^{-1}); C_a is the heat capacity of air (J m^{-3} K^{-1}); V is the vapour pressure deficit of the air (Pa); and r_a and r_s are the aerodynamic and surface resistances, respectively (s m^{-1}). Q_F represents anthropogenic heat flux, and Q^* and ΔQ_s refer to net radiant flux and storage, respectively. The equation is applicable to dry surfaces. If the surface is wet, the surface resistance r_s equals zero.

Evapotranspiration may be an important flux in urban areas, accounting for 22-37% of the daytime net all-wave radiation in residential neighbourhoods of a number of cities (Grimmond and Oke, 1998b) and 28-46% of the daily (24-hour) radiation. The evapotranspiration rates measured in downtown and light industrial sites are much less important. The authors note that evapotranspiration rates in residential neighbourhoods are almost independent of climate, since irrigation sustains evaporation in the absence of rainfall, even in desert cities such as Tucson. The limit on evapotranspiration in urban areas is therefore less likely to be related to the type of landscaping, and more to the extent of green space.

Figure 2.10: Relationship between average evapotranspiration at a site and fraction of the surface cover vegetated. ***(Grimmond and Oke, 1999b)***

The effects of vegetation in non-homogeneous areas

In a hypothetical homogeneous surface of unlimited horizontal extent, all of the fluxes would be perpendicular to the surface, i.e. vertical. However, the Earth's surface, and particularly urban areas, is a patchwork quilt of different surfaces. The horizontal inhomogeneity results in unequal fluxes of energy, and hence in advection. The effects of advection have been described in Section 2.5 above, but the special case of the effects of vegetation deserves a more detailed treatment.

As air passes from one surface type to another, climatically different surface, it must adjust to a new set of boundary conditions (Oke, 1987). The line of discontinuity is called the leading edge (Figure 2.11). The adjustment is not immediate throughout the depth of the air layer: Rather, it is generated at the surfaces and diffuses upward. The layer of air affected by the new surface is referred to as the internal boundary layer, and its depth grows with fetch downwind from the leading edge. Conditions are fully adjusted to the properties of the new surface only in the lower 10% of the internal boundary layer. The remainder of the layer is a transition zone where the air is modified by the new surface but not fully adjusted to it. The properties of the air above the internal boundary layer are determined by upwind influences and not by the surface immediately below.

Figure 2.11: The development of an internal boundary layer as air flows from a smooth, hot, dry bare surface to a rougher, cooler and moister vegetated surface *(Oke, 1987)*.

Urban areas are characterised by a variety of surfaces, and air passing over them is continually adjusting to the changing properties. Of particular importance is the adjustment that occurs when air passes from a dry, bare surface to a vegetated one (or vice versa), as illustrated in Figure 2.12 (Oke, 1987).

Figure 2.12: Moisture advection from a dry to a wet surface. (a) Evaporation rates and the vapour balance of a surface air layer. (b) Surface evaporation rate E_0, and mean water vapour concentration of the air layer. (c) Vertical profile of water vapour in relation to the developing boundary layer. ***(Oke, 1987)***

At the leading edge, assuming a two-dimensional flow perpendicular to the border between the two surfaces, the dry warm air induces a sharply increased rate of evaporation. If the vegetated surface is well irrigated, the 'edge effect' may result in evaporation rates substantially greater than the equilibrium rate over a saturated and extensive surface (Spronken-Smith et al., 1998). As air progresses downwind over the vegetated surfaces, its moisture content rises, gradually restricting the rate of evaporation until a new equilibrium is reached. The fetch required for the fully adjusted boundary layer to stabilize is typically about 100-300 metres for every 1-metre increase in the vertical. As the distance downwind from the leading edge increases and the internal boundary layer becomes thicker, the increase in moisture content of the air is diffused to a greater height. If the internal boundary layer is defined correctly, then the air above it experiences no increase or decrease in moisture, and advection results in horizontal convergence or divergence only.

Increased evaporation over a vegetated surface results in an increase in the latent heat flux and in a parallel decrease in the sensible heat flux. In extreme cases, a local surface-based inversion may be created. As the air approaches a new state of equilibrium in which evaporation is once again restricted (since the air is by

now moist), the sensible heat flux will once again increase gradually, until it too reaches a new equilibrium, at a rate that is somewhat lower than over the bare, non-vegetated surface. The air cooled by evaporation near the surface is gradually diffused, and the vertical temperature profile becomes more uniform compared with air over a bare surface.

Finally, if the vegetated surface is also rougher than the bare, exposed soil, the vertical profile of the wind will also adapt to the increased drag.

Figure 2.13: **(a) Adjustment of surface sensible heat flux and mean air temperature as air passes from a hot to a cooler surface. (b) Change in surface shearing stress and mean wind speed as air flows from smooth to a rougher surface. Associated modification of the vertical profiles of (c) air temperature, and (d) wind speed, at different distances downwind of the leading edge.** ***(Oke, 1987)***

The effect of trees on urban air temperature and surface energy balance fluxes

The presence of trees in the urban matrix may affect air temperature at a variety of spatial scales, from individual streets (Shashua-Bar and Hoffman, 2000) to city-scale modifications (Huang *et al*., 1987). However, the magnitude of this effect may depend on a variety of factors, because the interaction between trees and other constituents of the urban environment is so complex.

Oke (1989) summarised the energy balance of an urban tree as follows: During the daytime, the tree receives short wave solar radiation not only from the sky, but also radiation reflected from canyon walls and floor. Long wave radiation received is enhanced, because the tree is exposed to warm building surfaces that emit more radiation than the cool sky. In certain conditions, air temperature may be slightly warmer than the surface of the leaves, so the tree may also absorb sensible heat. The dissipation of this heat load depends on the water balance and wind climate of the tree. In the presence of unrestricted water, transpiration will cause substantial cooling. However, water supply to the root system may be restricted; stomata may be physically blocked by particulates; or the heat load may be excessively high, leading to closure of the stomata. Leaves also lose heat by long wave emission, especially from the upper part of the canopy exposed to the sky. Finally, temperature differences between the leaves and the ambient air are minimised by convection in the presence of strong wind. At night, there is no short wave load, and long wave radiation impinging on the tree canopy is also substantially lower than during the daytime. However, in the absence of sunlight there is no photosynthesis, so the stomata are closed and the tree is not cooled by transpiration.

The response of trees to increased energy loading, which may occur when individual trees are planted in extensive paved areas such as parking lots, for example, will vary with species, humidity of the atmosphere and how much of the crown is exposed (Kjelgren and Montague, 1998). Species from hot or arid habitats may be tolerant of high temperatures or able to dissipate heat with small leaves – but the evapotranspiration rates from such trees may be accordingly lower than those of broadleaf trees, and thus have a smaller effect on air temperature in their surroundings.

Grimmond *et al.* (1996) found that in a neighbourhood with a relatively dense tree cover, the latent heat flux increased as a fraction of available energy compared to an otherwise similar neighbourhood with a sparse tree cover, as did the storage flux, whereas the sensible heat flux decreased. However, in absolute terms, all fluxes, including the sensible heat flux, were enhanced at this neighbourhood. Trees and shrubs lowered the albedo and surface temperatures, thereby reducing the loss of solar and long wave radiation, respectively – resulting in an increase in the overall amount of energy to be dissipated compared to the sparsely planted neighbourhood. As a result of the difference in fluxes, the maximum air temperature above the canopy was about 1 ^{o}C higher in the densely planted neighbourhood, while temperatures below the trees at noon and in the early afternoon were similar or up to 0.5 ^{o}C higher than in the sparsely planted neighbourhood.

In contrast to Grimmond *et al.* (1996), most researchers report that trees reduce urban air temperature. This is usually attributed to evapotranspiration, but Shashua-Bar and Hoffman (2003) suggested that the cooling

is due almost entirely to shading, which more than offsets the exchange of sensible heat between the tree canopy and the air. Shashua-Bar and Hoffman (2002) proposed a quantitative model for predicting the cooling effect of trees in an urban setting, but their method incorporates site-specific empirical factors to account for convective exchange, the magnitude of which is not systematic and for which there is no method of calculation. The method is nonetheless demonstrated in an empirical study of the effect of trees on air temperature in the streets of Tel Aviv, Israel, which found that the overall cooling effect of trees could be as high as 3 K, depending in addition to the shade coverage on the depth of the urban canyon, albedo of canyon walls and on street orientation (Shashua-Bar and Hoffman, 2004).

The park cool island (PCI)

The effect of local parks in a non-homogeneous urban area has been the subject of intense study, especially once it became clear that the microclimate of built-up areas differed substantially from that of rural areas. The so-called *park cool island* (PCI), a manifestation of the more general *oasis effect*, is the converse of the urban heat island (UHI): Empirical findings show that air temperature in moderate to large-sized parks may be substantially lower than temperature in surrounding built-up areas (Kanda and Moriwaki, 1998). Data from Mexico City (Jauregi, 1990-91) showed that temperatures in a large urban park (area ~500 ha) were as much as 4 ^{o}C cooler than in neighbouring areas, the maximum difference typically occurring in the dry season, just before sunrise. Daytime maxima were, however, similar, the park often being slightly warmer (about 0.5 ^{o}C) than its urban surroundings. The effects of the park cool island beyond the vegetated area were felt up to a distance that is approximately equal to the width of the park itself.

Spronken-Smith and Oke (1998) distinguished between surface temperature PCIs, which may be quite large, and air temperature PCIs, where the effects of surface temperature variation are diluted by near-surface turbulent mixing and advection by wind. During daytime, surface temperatures are affected by the presence or absence of shade, by surface albedo, by water availability and by the thermal properties of the soil. These properties govern the receipt of solar radiation, its absorption and the role of evaporative cooling. At night the thermal properties of surfaces and the radiative geometry are the major controls on cooling. Urban parks vary substantially with respect to the above factors, and may be classified according to the arrangement of vegetation (Spronken-Smith and Oke, 1998): Grass; grass with tree border; savannah (grass with isolated trees); garden; forest; and multiuse.

Park cool islands may develop either during the daytime, or at night. However, a given urban park will display a regular diurnal pattern, indicating that the formation of PCIs may be the result of a number of mutually exclusive factors. Spronken-Smith and Oke (1999) found that daytime PCIs formed as a result of the combined effects of soil moisture and shading: Trees shade the surface, while grass is typically cooler than most solid surfaces during the daytime, if it is well-irrigated. The relative coolness of irrigated parks therefore peaks in the afternoon (forest type), or early evening (garden, savannah and multiuse types). However, trees also inhibit nocturnal long wave radiative cooling by blocking off part of the sky, while excess moisture increases the thermal capacity of the soil and slows down surface cooling. Night-time PCIs therefore typically

form in relatively dry urban parks with a sparse tree cover. They are driven by long wave radiative cooling (since the sky view factor is close to unity), and since evaporative fluxes are generally weak at night, evaporation does not play a significant role in the formation of this type of PCI. In such parks, daytime temperatures may sometimes be higher than in neighbouring urban areas. However, there exists an 'edge effect' that applies within distances of about 2.2-3.5 times the height of the park border, and which results in weaker radiative cooling where the sky view factor is reduced by the obstructing features, such as perimeter trees or buildings.

The contrast between the dry surroundings and extensively irrigated urban parks creates a number of interesting phenomena:

- The '*oasis effect*' is a local-scale phenomenon in which evaporation is enhanced as a result of mechanical subsidence of warmer regional (city) air down over the cooler park due to mass divergence within tens of metres. If water supply is not restricted, the extra downward flux of sensible heat supplements the radiative energy supply and permits abnormally high rates of evaporation. In an oasis formed as a result of agricultural land use in China, a daytime inversion layer about 8 metres thick was recorded (Kai, 1997). Air temperature near the surface was about 2 ^{o}C lower than temperature at the top of the inversion layer, which was typically observed during the afternoon of fair weather days, when the wind from the surrounding desert was fairly strong.
- The '*thermostat effect*' is a phenomenon first observed with respect to leaves, and refers to the tendency of a wet surface to maintain an almost constant temperature in an increasingly hot environment, at temperatures of 30-35 ^{o}C or more. Spronken-Smith *et al* (1998) reported that an extensively irrigated urban park may act like a giant leaf: as air temperature increases and approaches its daily maximum, the temperature difference between the air and the ground surface decreases, and the ground may be even be slightly cooler than the air near the time of peak heat input ($Q^{*}+Q_{H}$). However, since some of energy required to evaporate water is sensible heat introduced from adjacent areas by advection, the process does not occur in the absence of wind, and as a result the temperature of air 1 metre above the surface of the park and above adjacent paved areas is very close – surface temperature differentials in excess of 15 ^{o}C notwithstanding.

The extent of vegetated area required to produce measurable effects on air temperature is of great interest to urban planners. Saito et al (1990-91) reported cool islands in clumps of vegetation less than 200 metres across, but the effect of vegetation was limited to the planted area itself, and was not felt at distances as little as 20 metres away from the park edge. Shashua-Bar and Hoffman (2000), who reported differences of up to 3 K between air temperature in tree-shaded urban avenues and nearby, non-shaded reference points, when wind speed was very low, noted that the cooling effect declined at an exponential rate with increasing distance from the border of the planted area, and vanished less than 100 metres away from the sites studied. Numerical modelling (Bruse and Fleer, 1998) indicates that small parks of only tens of metres across may create temperature differentials of 2 ^{o}C or more. However, the horizontal gradients of air temperature

represented by the models may be quite large, and their spatial patterns shift constantly with wind speed and direction. The usefulness of such models may lie simply in exposing the fact that such variations exist, rather than in application of their predictions.

The effects of vegetation on building energy consumption

Landscaping and careful planting of vegetation near buildings have been credited with energy savings of anything up to 80% in hot, dry climates (Meier, 1990-91). Whereas McPherson *et al* (1989) suggested that the localized effects of vegetation on building microclimate may be more significant than boundary layer effects, Ca *et al* (1998) reported on the basis of measured data that an urban park 0.6 km^2 in area can reduce air temperature in a commercial area 1 kilometre downwind by as much as 1.5 ^oC. However, much of the evidence remains anecdotal.

The mechanisms by which vegetation affects the energy exchange between buildings and the environment may be summarised as follows:

- Vegetation can reduce energy consumption in building in hot climates if *air temperature is reduced* near the planted area. The energy savings depend not only on the drop in temperature, but also on the spatial extent of the cooled area. However, it should be noted in this context that heat transfer through building walls is driven by differences in surface temperature, rather than air temperature. Furthermore, the reduction in air temperature resulting from evapotranspiration is accompanied by an increase in the vapour content of the air. Therefore, the air conditioning system must deal with an increased latent heat load, offsetting to some extent any gains from a lower sensible heat load.
- Plants may *shade building surfaces,* reducing the radiant load on the envelope. This may be beneficial in hot climates, but detrimental in cold ones. In temperate climates with distinct heating and cooling seasons, deciduous trees are often planted, and vine-covered trellises are common in many Mediterranean areas. However, the timing of defoliation and the permeability of the bare trees vary widely from species to species (Canton et al., 1994) and may not match the desired pattern of exposure to the sun. McPherson *et al* (1988) found that in the middle latitudes, cooling loads were most sensitive to shading on the roof and on the west wall, while heating loads were affected most by exposure of the south (equator-facing!) and east walls.
- Plants may *reduce wind speed* near buildings, limiting unwanted infiltration, but also restricting ventilation and reducing convective exchange at building surfaces. The first two mechanisms are self-explanatory, but the third has less well-known consequences. For instance, in hot climates, wind is an asset for unshaded houses because it helps remove radiant heat at the external building surfaces (McPherson et al., 1988), reducing temperature differentials between interior and exterior. However, in poorly insulated houses, especially in cold climates, increased convective exchange at the building envelope results in increased loads on building heating or cooling systems.

- Plants may *reduce temperatures of ground surfaces* by evapotranspiration (in warm conditions only – planted surfaces may be warmer than bare soil in cold climates!), having two effects: Cooler surfaces emit less infra red radiation, thus reducing the radiant load on building surfaces; and they release less heat sensible heat to the adjacent air, so that buildings are exposed to cooler ambient air. The cooling effect of a well-watered lawn may be quite substantial: Zangvil (1982) showed that in desert conditions, air temperature 2 metres above the grass may be up to 6 ^{o}C cooler than above bare soil, for a range of wind speeds.

The direct effect of shading building surfaces by plants was studied by Papadakis *et al* (2001). Thick foliage producing a full shade effect resulted in a reduction of the surface temperature of a light-coloured concrete wall by up to 8 ^{o}C, with concomitant reductions in heat flux through the surface. When wind speed was negligible, air moisture content in the planted canopy was up to 2 g m^{-3} greater than in the surrounding air. Likewise, a dense growth of ivy can block radiant exchange at the wall surface almost entirely (Hoyano, 1988). However, several studies show that where the shaded area has a limited spatial dimension - for instance beneath a pergola (Hoyano, 1988) or in the shade of a liman (small clump of trees in an artificial flood-plain in the desert) (Schiller and Karschon, 1974) - the effect on air temperature at a height of as little as 1 metre above the ground is negligible.

Roof gardens (or planted roofs) are perhaps the most obvious example of the use of plants to control building energy performance, and are sometimes credited with improving the urban microclimate as well (Wong et al., 2003). The shading and evapotranspiration of the plants contribute to lower surface temperatures and thus to lower heat gains through the roof. Much of the work in this field is empirical and lacks a comprehensive theoretical framework (Niachou *et al*., 2001). Experiments show that the surface temperature of an exposed roof can be reduced substantially by the addition of an irrigated lawn on a fabric matrix (Onmura *et al*., 2001). A complete thermal model of a planted roof (Palomo Del Barrio, 1998) showed that the contribution of the planting to the thermal performance of the roof depends mainly on the density of the foliage, the water content present in the substrate, and the composition, density and thickness of the substrate. However, unless the thermal conductivity of the soil is particularly low or the thickness of the substrate is considerable, the thermal resistance provided by the planting and substrate is usually insufficient during the cold season even in mid-latitude countries with relatively mild winters.

Various studies have been carried out to investigate the direct effect of vegetation on energy consumption in buildings, in addition to its more general role in modification of the microclimate. Several approaches have been proposed, including comparative measurements of energy consumption of similar buildings in different landscapes and computer modelling of the shading effect of trees and their effect on wind speed.

A model specifically designed to predict the general microclimatic effect on energy consumption of augmenting urban vegetation was proposed by Sailor (1998). The mesoscale model (2 km x 2 km grid) predicts that by increasing the vegetated fraction of the core of a hypothetical city by 0.065, annual cooling loads could be reduced by 3-5%, simply by the lowering the background air temperature. The model was

tested on the basis of data from several cities in the United States, located from 25°N latitude to 45°N latitude.

Simpson and McPherson (1998) attempted to quantify energy savings resulting from planting trees in a city (Sacramento, Calif.) by calculating the effect of shading on buildings, with respect to summer (reduced radiant load resulting in lower cooling costs) and to winter (reduced solar penetration resulting in increased heating costs). The calculation was done on the basis of building energy simulation for a typical construction (slab-on-grade, timber frame; insulation according to State standards prevailing at time of construction). Actual building sizes and trees were used in a sample of about 250 houses. Cost savings of approximately $14 per tree per annum were calculated – although no account was made of general microclimatic modifications resulting from the intensive planting campaign carried out in the city. The study was followed up by a more systematic attempt to analyse the effect of trees according to type and location with respect to the building (Simpson, 2002), providing a set of look-up tables to assist in manual assessment of the effect on building energy consumption.

2.8 Deliberate modifications to the urban microclimate

Study of the urban microclimate is driven, among other reasons, by the desire to modify meteorological conditions in cities in a deliberate manner, to achieve a variety of goals. These include the creation of (thermally) comfortable outdoor spaces and energy conservation in buildings.

The importance of environmental factors in the design of settlements was recognised at least as early as Roman times, as recorded in the writings of Vitruvius, who warned planners, for example, that "if the streets run straight in the direction of the winds then their constant blasts rush in and sweep the streets with great violence" (Vitruvius, 1999). However, most settlements (to this day) are either not planned, or their planners have little consideration for climatic factors. Page (1968) identified three reasons why scientific information available to researchers would nonetheless be rejected by practitioners:

1. The potential user considers the information provided irrelevant.
2. The user considers the information provided inapplicable in the form presented.
3. The user considers the information provided incomprehensible.

Page noted that in order to be of use to urban planners, urban climatology must first be predictive – descriptive science was not in itself sufficient. Furthermore, the problem was not to produce an idealised climatological plan, but to produce a workable evolutionary plan that is economically viable and accepts that the planner must consider other factors, such as land values.

In a subsequent article, Page (1972) listed the following facets of urban design that he considered sensitive to climate:

1. Optimisation of land-use patterns in relation to different activities to be carried out in the town
2. Identification and development of suitable microclimates for various activities, such as parks or recreation
3. Identification of adverse microclimatic factors likely to affect the detailed design of urban systems, such as high local winds
4. Optimisation of building form in relation to external climatic inputs, such as solar radiation and wind
5. Optimisation of building form in relation to microclimatic modification of the immediate exterior domain of the building, such as the high winds induced near ground level by tall buildings
6. Constructional safety, especially with respect to high winds
7. Selection of appropriate building materials
8. Planning of the construction process itself in view of climatic constraints
9. Control of water runoff
10. Assessment of building running costs (HVAC, lighting, etc.) in advance of construction
11. Optimisation of the operating environment of transport systems, for example: avoidance of ice hazards
12. Control of the environmental impact of a transport system on its adjacent urban systems, for example with respect to air pollution by vehicles

There is growing awareness of the importance of climatological inputs in the process of urban planning. However, a recent study (Eliasson, 2000) showed that even in Sweden, where environmental concerns are the subject of much public debate and where urban planners are interested in climatic aspects of design, the use of climatic information is not systematic and climatology has little impact on the planning process. The reasons for these are not only conceptual and knowledge based, but also related to technical matters, policy issues, organizational aspects and the market.

Climatic considerations have nonetheless had a major effect on the plans of a number of new neighbourhoods or towns (Gotz, 1982; Etzion, 1990; Evans and de Schiller, 1990-91; El-Shakhs, 1994). However, in all of these cases, planning decisions were made on the basis of an intuitive understanding of local conditions, and not on the basis of scientific analysis of the meteorological conditions and likely urban effects. The only variable sometimes treated in a quantitative manner is solar access rights (to direct radiation), based on geometric considerations of apparent solar position.

Unfortunately, most publications on application of urban climatology to the planning process fall into one of two categories: They are either cases studies of conditions in existing settlements (Potchter, 1988); or they provide only general recommendations, but no quantitative guidelines and no design tools (Landsberg, 1968;

Golany, 1996). Borve (1982), Westerberg and Glaumann (1990/91) and Pressman (1996) offered such guidelines for so-called 'winter cities'; Aynsley and Gulson (1999) proposed design strategies for humid tropical cities in general, while Emmanuel (1995) suggested strategies specific to Colombo, Sri Lanka; Herz (1988) drew up recommendations for the Sahel region.

There have been several attempts to establish a consistent quantitative framework through which urban climatology could be used to improve urban planning. One early example of such an attempt modelled not only the urban microclimate, including air temperature and the wind field, but also energy consumption in buildings (Rauhala, 1984). However the author recognized that in view of the limited capabilities of computers at the time, the model required several simplifications that could lead to erroneous results.

Oke (1988a), with mid-latitude cities in mind, proposed the following objectives for urban planners considering an appropriate response to climate:

- To maximise shelter
- To maximise dispersal of pollutants
- To maximise urban warmth
- To maximise solar access

Considering the aspect ratio of streets as the only parameter to be modified in order to achieve those objectives, Oke suggested that a height to width ratio H/W=0.4 was a compromise that would lead to satisfactory performance with respect to all of them. However, the limitations of this approach are evident when the implications of relatively low density are explored in the context of air quality and overall energy use in a hypothetical study of Melbourne (Manins *et al*., 1998), which found that a compact city performs best on a number of measures. The study did not consider alternative morphological solutions for achieving the specified densities, and the field is one that will support extensive research.

Solar exposure

A primary concern of many planners in (relatively) cold climates has been to maximise solar exposure of buildings, to permit passive solar heating. This aspect of urban planning has generally been investigated in isolation from other aspects of urban climatology, not least because it only requires knowledge of geometry. Littlefair (1998) surveyed a variety of graphic methods to establish solar exposure, though a substantial number of CAD programs now perform the task automatically, given a geographical location and time of year. However, the study raises the intriguing question of how to establish the criteria for solar exposure. It proposes that rather than mandate solar access on the winter solstice, when the sun is lowest, it may be preferable to define a heating season and aim to maximise gains over the whole period. Meeting the first requirement in high latitude locations requires exceedingly large distances between adjacent buildings in order to provide what may be marginal benefits, because sunshine hours are short and insolation is limited.

Guaranteeing exposure when insolation levels are higher may fill a proportion of heating requirements that is only slightly smaller yet requires far less stringent geometric limitations on building height.

In tropical climates, in contrast with cold climates, exposure to solar radiation is generally undesirable. Planners in such locations are therefore concerned with creating urban geometries that maximize shade. Unlike the narrow streets and a dense urban matrix sometimes recommended for desert locations but which restrict ventilation (Mazouz and Zerouala, 1998), designs for warm humid locations must maximize air flow yet provide shade in public spaces of relatively low-density tropical cities (Emmanuel, 1993).

In temperate climates, design for solar access reflects a desire to accommodate sometimes-contradicting requirements in response to seasonal weather and solar exposure. Swaid (1992) proposed that operable screens be installed on building rooftops to restrict solar access into street canyons when radiation is excessive, yet which are capable of being folded away when full exposure is desirable. The effect of adjustable screens on canyon air temperature was simulated, and significant differences were reported among the different configurations tested.

Several studies on the orientation of streets, usually in a grid scheme, have recommended various orientations on the basis of exposure of buildings or of street surfaces to direct solar radiation. Gupta (1984) defined efficiency factors for building form on the basis of protection from solar radiation in hot climates, and a combination of winter exposure and summer protection for composite climates. The effect of an urban matrix comprising linear streets, stand-alone pavilions or square courtyards was assessed for different solar geometries and various orientations, and recommendations made regarding the preferred urban form. For example, in composite climates, an east-west street with continuous wall surfaces was found to be the optimum configuration (from building-energy considerations), but in low-latitude locations, a north-south street axis gave buildings equal solar protection to an east-west oriented street. A similar study (Mills, 1997a) compared the effect of building group configuration on the thermal stresses affecting individual buildings, on the basis of two measures: solar exposure (controlling heating) and sky view factor (controlling cooling by long wave radiation). The study provides a useful insight into the effects of urban geometry, but recommendations for different climate zones (defined by latitude) are of necessity too simplistic, not least since they ignore the effects of convection on building energy needs.

Considering solar exposure of streets, rather than buildings, Knowles (1981) arrived at different conclusions: a ‘Spanish grid’ (in which streets are oriented at 45^{o} to the cardinal points of the compass) was found to be preferable to the so-called ‘Jeffersonian grid' (in which streets are oriented east-west and north-south). This is because in the Spanish grid, part of the street is shaded while the opposite sidewalk is exposed to the sun all year round, allowing pedestrians to choose between different conditions. The Jeffersonian grid, in contrast, maximizes mid-day exposure on the north-south streets in both summer and winter, while east-west streets will be in shadow most of the time in winter, unless they are very wide, and exposed to the sun during summer. Shashua-Bar and Hoffman (2003) pointed out, correctly, that extensive planting of trees minimizes the effect of street orientation with respect to solar access. However, the question of street orientation should

be considered not only from considerations of solar access (or protection), but also with respect to wind direction, especially where lack of ventilation is a major problem (Ahmed, 2000).

Mitigating the urban heat island

The urban heat island is not necessarily detrimental, especially in cold climates. However, in warm-climate cities, there are compound benefits from a reduction in surface and screen level air temperatures (Taha *et al*., 1997). The potential benefits include, in addition to a decreased demand for cooling energy, a decrease in some photochemical reaction rates and thus lower ozone levels, a decrease in temperature-dependent biogenic hydrocarbon emissions from vegetation and a decrease in evaporative losses. However, any strategy to mitigate heat islands should be evaluated in the context of complex inter-related effects of the varied controls on the urban microclimate.

Many consider controlling solar gain as the first step in planned modification of the urban microclimate. Bretz *et al.* (1998) suggested that solar reflective (high-albedo) alternatives to traditionally absorptive surfaces such as rooftops and roadways can reduce cooling energy use at almost no cost. All else being equal, the application of high-albedo materials reduces the temperature of surfaces exposed to direct sunlight by reducing absorption of solar radiation. The main effect may be observed during the daytime, when high surface temperatures result in greater sensible heat flux and thus elevated air temperature, but residual effects may be felt throughout the diurnal cycle as energy stored in the substrate is gradually released. Taha *et al.* (1997) found, using the CSUMM mesoscale model, that feasible albedo changes could lower daytime maximum temperatures in central Los Angeles by up to 2 ^{o}C, with smaller reductions predicted for the suburbs. The scale of modification possible depends on the area of solid surfaces such as rooftops, streets and other paved areas as a proportion of the total urban area. Based on study of aerial photographs, Bretz *et al.* (1998) found that in Sacramento, California, such surfaces comprised a total of 58% of the city, compared with 42% for planted areas, and the overall increase in albedo resulting from the use of reflective materials on these surfaces was calculated to be 18%. The actual energy savings obtainable from the use of high-albedo materials in roofing and/or in paving materials depend not only on the resulting modifications to the urban air temperature, but also on the thermo-physical properties of the buildings. Taha *et al* (1988) suggested that reductions in cooling energy in Sacramento, California, could be on the order of 62%, with 44% fewer cooling hours and 35% lower peak power demand. The results of the simulation are sensitive to various inputs, some of which may not be realistic, such as a house albedo of 90%. However, the potential for affecting energy consumption on an urban scale clearly exists.

Landscaping, specifically the incorporation of planted areas in the urban fabric, seeks to minimize differences between natural terrain and the urban surface. Bonan (2000) demonstrated in an empirical study of a town that “in the semi-arid Colorado environment, the choice of planting material, the design of irrigated greenbelts within a community and the density of housing all have important consequences in creating thermally pleasing environments”. However, the same study found a substantial difference between the behaviour of an irrigated lawn and that of a non-irrigated grassy area: the availability of water and the resulting increase in

evaporation was the main factor responsible for lower surface temperature and air temperature above the lawns, rather than the mere presence of plants. This helps to explain the finding that increasing the proportion of planted areas in a city tends to reduce daytime maximum temperatures, but has little or no effect on night-time minima (Urano *et al*., 1995). Emmanuel (1997) noted that the main effect of trees is to reduce radiant exchange at the ground surface: This may reduce daytime maximum temperature, but would also restrict nocturnal cooling, leading to higher minima. A mesoscale model used to evaluate the effect of vegetation on air temperature in a hypothetical city highlighted the effect of soil moisture availability (Sailor, 1998). Increasing moisture availability by 0.15, leaving all other parameters in the model unchanged, resulted in a decrease of 19% in cooling degree days (CDD) and an increase of 6% in heating degree days (HDD).

Dhakal and Hanaki (2002) carried out a quantitative numerical analysis of strategies for reducing the UHI in Tokyo. The analysis was carried out using the CSUMM meso-scale climate model, with inputs describing real buildings in Tokyo from a detailed GIS database and a DOE 2.1 simulation of heat flux in typical building types. Strategies for urban intervention investigated included: 1) Changing location of HVAC heat exchangers (roof, ground etc.); 2) Changes in the type of air conditioning systems (e.g. introduction of heat pumps or cooling towers); 3) surface modification (e.g. increased albedo of roofs, roads etc.); and 4) introduction of vegetation. The maximum improvements (reduction of UHI) predicted were about 0.5 ^{O}C during the day, and only 0.1 ^{o}C at night. The energy-related scenarios led to reductions in night temperatures but had little effect on daytime peaks. The surface related strategies, especially the introduction of vegetation, had little effect on night temperatures but resulted in substantial daytime modifications. A major drawback of the methodology was, however, the fact that the CSUMM meso-scale model is not specifically adapted to urban conditions, and does not simulate the urban canyon as such.

Ventilation

Adequate ventilation is necessary not only to remove pollutants and excess heat from urban sources, but also to improve human thermal comfort in warm humid climates by increasing the rate of convective heat loss at the skin and by evaporating perspiration more effectively. Promoting exposure to regional winds on an urban scale has been an aim of city planners from ancient times (Kenworthy, 1985). However, the means of doing so are not clear. While streets oriented parallel to the prevailing winds would appear to offer the least aerodynamic resistance, Kenworthy found in scale-model tests of orthogonal block grids that the maximum wind speed at street level was measured when the wind blew at a small angle to the main axis.

2.9 Summary

This chapter has reviewed the main forces that modify the urban microclimate and which are responsible for urban-rural differences. Where possible, quantitative models have been introduced that describe each of the physical processes involved. These are incorporated in an energy balance equation that includes radiant heat transfer, storage, turbulent flux (both sensible and latent), and anthropogenic heat.

While our understanding of the effects of the built environment on each of the above mechanisms is fairly clear, the complexity of the urban canopy layer is such that modelling the interactions of these mechanisms remains a challenge. And though the principles may be well established, our capacity to describe the processes in sufficient spatial detail for meaningful periods of time is still limited, especially the complex effect of the urban environment on wind. The lack of sufficiently detailed databases of actual cities, especially with respect to the distribution of sources of anthropogenic heat, is a further handicap.

The following chapter will review a variety of frameworks that have been devised to bring together some or all of the forces at work with the intention of creating a complete model of the urban microclimate. It will then propose a new modelling framework that is subsequently translated into a computer program that simulates conditions in an urban street canyon on the basis of measured reference data.

CHAPTER 3: MODELING APPROACH

3.1 Modelling the Urban Microclimate

Urban climate models, whether physical or mathematical, may be used to investigate the urban climate at different scales. These range from meso-scale models that simulate the conditions in the planetary boundary layer (PBL) above cities, such as URBMET (Bornstein, 1975), through models of an intermediate scale (Mills, 1997b) to micro-scale models of the urban canyon (Arnfield, 1990). The micro-scale models may be coupled to the meso-scale ones, as in (Taha, 1978), or they may be independent (Swaid and Hoffman, 1990c). The type of model used is determined by the purpose for which it was created.

Most models are designed to investigate and interpret specific features of the urban environment. Often a one-dimensional representation or 2-D models are sufficient. However exploration of urban effects with a definite spatial differentiation requires both a system for describing the heterogeneity of the city in a meaningful manner, and a means of assembling the necessary information.

Ellefsen (1990/91) proposed a system for classifying all urban buildings into 17 categories, grouped into three types of zones: Attached buildings, detached building (close-set) and detached buildings (open set). The classification scheme was based on a very detailed study of building stock in ten US cities, and included parameters such as street pattern, lot configuration, building placement on the lot, building density, building construction type and age of construction. In addition, the system can incorporate details such as construction materials. Grimmond and Souch (1994) presented a methodology that uses GIS to represent the urban surface in a more general approach, which is not restricted to the properties and morphology of buildings. The procedure may be used to describe a site objectively, model fluxes or ensure spatial consistency between measured and modelled data.

Field studies

Observation and measurement may provide direct evidence of a phenomenon being studied, and are often the first indication that a process of interest is occurring. Monitoring of environmental conditions in the field requires a number of formidable obstacles to be overcome:

- The time scale during which monitoring is carried out must be appropriate for the phenomenon being studied. For instance, analysis of changes in climate requires records covering decades or even centuries.
- The spatial resolution and extent of the monitoring system must be appropriate. The site characteristics should be described accurately so that it is clear what the measured data represent.

- The accuracy of the sensors used should be sufficient to record changes in the property being measured (generally by an order of magnitude).
- The properties being measured should take into account all factors affecting the process under investigation.

The complexities of the urban environment have made field studies of microclimate in the city very difficult. The ability to reach generalized conclusions with respect to a phenomenon being studied is limited by the peculiarities of individual sites, such as the random effects of the local wind field, specific details of building morphology or the effects of a particular arrangement of plants. Nevertheless, if the site is described accurately, it may be possible to gain useful information from field studies.

Numerous field studies have been dedicated to various aspects of the microclimate of the urban canopy layer. Of particular importance in this context is the study by Nunez and Oke that first established the urban canyon as the basic unit of study of meteorological conditions in the city (Nunez and Oke, 1977). Detailed measurements of energy fluxes from canyon surfaces and of net radiation at various heights above the canyon floor provided the basis for the first energy balance calculations for a dry canyon.

The urban canyon has been the focus of numerous field studies in the ensuing years. Following Nunez and Oke, additional measurements of the energy balance have been carried out by Yoshida *et al*. (1990-91). A study by Arnfield and Mills (1994b) highlighted the difficulty of resolving the interface between the canyon and the urban boundary layer above. Other studies have been devoted to specific processes, such as long wave radiation (Nunez and Oke, 1976), the urban water balance (Grimmond and Oke, 1986), heat storage (Grimmond and Oke, 1999c) and the effects of vegetation (Jauregi, 1990-91; Grimmond *et al*., 1996). Numerous studies have concentrated on the effect of buildings on air flow, often seeking to correlate the attenuation of wind speed in the urban canyon relative to wind speed above the roof with canyon geometry (Nakamura and Oke, 1988; Johnson, 1990; Johnson and Hunter, 1999).

Field studies of meso-scale effects of cities on conditions in the urban boundary layer require measurements to be made above the canopy layer. Many of these studies were designed to assess the aerodynamic roughness of the city, and specifically to determine the roughness length and zero-plane displacement (Grimmond *et al*., 1998). Measurements of fluxes of energy and momentum are usually carried out on tall masts, so that the instruments are in the inertial sublayer (also known as the constant flux layer), where changes in the magnitude of the flux due to change in measurement height are considered negligible (less than 10 percent) of the change resulting from horizontal location.

Other studies have been carried out in order to map variations in meteorological parameters over the urban area. Most such studies have mapped variations in air temperature, by means of mobile traverses (Saaroni *et al*., 1999) or numerous fixed stations (Santamouris, 1998). Of particular interest in this context is the use of remote sensing to obtain thermal images of large areas concurrently. The camera may be mounted on an airplane (Hoyano, 1984; Ben-Dor and Saaroni, 1997; Voogt and Oke, 1998), or on a satellite. The level of

detail may be quite fine – features as small as 5 m may be identified clearly (Quattrochi et al., 1998; Quattrochi and Ridd, 1998). This allows analysis of the thermal response of discrete patches of surface in correlation with earth-based sensors. It should be emphasized that remote sensing techniques produce an essentially two-dimensional representation of the three-dimensional urban surface, albeit one that comprises those surface elements that are most exposed to the sky.

The use of remote sensing, typically satellite-based, has a number of advantages over land-based or airborne systems: 1) Satellites usually employ multi-spectral sensors that permit simultaneous scanning of different properties of the same surface area; 2) Satellites offer simultaneous coverage of large areas (albeit typically at the expense of resolution); and 3) Satellites may be used to repeat scans of areas under study at extended intervals without requiring complex organization to set up the necessary sensors. This simplifies the process of investigating changes over time, such as the process of urbanization of a previously rural area (Carlson and Arthur, 2000).

Physical models

Physical scale-models are typically used to isolate and analyse the effects of a particular climatic process when it becomes necessary to validate a numerical model or a component of such a model, or to reduce the inherent diversity encountered in real urban environments. Scale models may be studied in laboratories, under controlled conditions, but a number of experiments have been conducted where scale models have been exposed to the natural environment. Scale models need to address issues of similarity and scaling, and even when these are resolved in a satisfactory manner are generally incapable of reproducing the complex interactions between the various environmental processes.

A scale model was first used in urban climate research to investigate the urban heat island occurring in the city of Fort Wayne, Indiana (Davis and Pearson, 1970). A model of the city comprising 17,000 individual elements was constructed of building lathe, and placed in a flat, open field. The horizontal and vertical scales of the model were not identical, a distortion deemed necessary by the roughness of the surrounding terrain (grass). However, issues of scaling were deemed to have been resolved satisfactorily, and the authors concluded that the model demonstrated the feasibility of using the real atmosphere as a medium in which to conduct meteorological modelling experiments. Changes in stability resulting from the model geometry were recorded, and a small heat island was measured.

Several studies have incorporated reduced scale physical models to investigate the effects of urban form on radiation exchange, including two of the most influential studies in urban climatology – by Oke (1981) and Aida (1982). Such models are necessary because there are inherent difficulties in performing accurate and representative radiometry of urban surfaces. In order to sample a sufficiently large source area, aircraft or satellite borne instruments are required. The procedure is not only expensive, but is incapable of performing continuous measurements over an extended period of time. Furthermore, allowance must be made for atmospheric absorption and for flux divergence between the terrestrial surfaces and the airborne sensor. The

extremely varied geometry and materials of the source areas are rarely described adequately, making generalization difficult.

The effect of urban form on long wave radiative exchange was studied using a scale model in a climate chamber where all other forms of heat exchange were either neutralized or accounted for (Oke, 1981). The cooling rate of a small model city (0.5 metre square base, with streets 50 millimetres wide) constructed of wood was found to be inversely related to the canyon aspect ratio (H/W), providing the physical basis for a phenomenon observed in many cities showing that night-time temperatures in dense urban centres were substantially higher than those in open ('rural') locations. The same model was later developed to account for evaporative effects through the creation of a central 'park' with soil of various moisture contents simulated by a porous material and scale-model trees added to investigate the effect of plants at different densities on radiative exchange (Spronken-Smith and Oke, 1999).

The effect of morphology on the albedo of a city was established by means of a scale model consisting of cubic concrete blocks 15 centimetres a side placed on the roof of a building (Aida, 1982). Results of this experiment suggest that annual albedo for a city located at 35 degrees latitude could vary between 0.23 and 0.4. A numerical model developed following this experiment (Aida and Gotoh, 1982) found that the maximum absorption occurs when the canyon width is approximately twice the block width.

The relationship between nocturnal long wave radiation and urban surfaces in the city was investigated in several experiments: Voogt and Oke (1991) constructed a simplified scale model of a street consisting of two parallel walls 10 metres long and 1 metre high to validate a numerical model proposed previously (Arnfield, 1982); Swaid (1993b) modelled an urban canyon using polystyrene boards 63 centimetres wide and 2.5 metres long, and varied the spacing to simulate canyons of different widths.

Wind tunnel studies have often been used to model the dispersal of pollutants (Kastner-Klein and Plate, 1999) or to provide the basis for engineering calculations of wind loads on buildings. In the context of urban climatology, the combined effect of the urban heat island (UHI) and the urban roughness island (RI) create a substantial disturbance to the approach flow. In order to allow accurate modelling of urban-scale effects, it is necessary to ensure similarity of the model and of the real environment in two respects (Cermak, 1995): similarity of the approach flow, dealt with by appropriate design of the upwind fetch; and similarity of the mechanical and thermal features of the model and the urban area. In aerodynamic terms, this requires equality of the Richardson numbers of model and real environment, Reynolds number sufficiently large to realize Reynolds number independence, flow distance sufficiently long to develop boundary layer in equilibrium with surface roughness and temperature and a zero longitudinal pressure gradient. Plate (1999) discussed the advantages of boundary layer wind tunnel studies using physical scale models and compared them with mathematical models.

A recent study using boundary layer wind tunnels (BLWT; also referred to as meteorological wind tunnels) has shown that building spacing has a smaller effect on roughness, wind retardation and turbulence than roof

shape (Rafailidis, 1997). A simple model deriving the mean canopy velocity profile from the overlying semi-logarithmic wind profile was proposed on the basis of a study using simplified urban forms in a wind tunnel (Macdonald, 2000). The model incorporates an attenuation factor that is related to the density of the urban form, but the result is currently limited to situations where the frontal area density is less than 0.3, and is thus inappropriate for most city centres. Numerous wind tunnel studies of specific configurations of building height, staggering etc., such as Alberts (1982) and Al-Sallal *et al.* (2001), give essentially qualitative results that may be useful to planners but generally have no quantitative application.

The development of the urban heat island may also be studied in a convection tank, with water as the working fluid. Lu *et al.* (1997) maintained that the water tank is a suitable tool to study the evolution of a thermal plume above the city on a meso-scale, even though the geometric structure of the buildings was not reproduced and the regional flow was not simulated.

Mathematical (analytical) models

Field studies are lengthy, expensive, and often very difficult to interpret. Furthermore, they can only be used to study existing situations, and have no predictive capacity. Physical models may be useful, but are generally incapable of reproducing exactly conditions in the field, and may be difficult to extrapolate to the variety of desired conditions. There is thus a need for mathematical models, in the study of urban climatology as in other fields.

Mathematical models are generated on the basis of analyses of the environmental processes that contribute to the microclimate in a given location. Bornstein (1984) suggested three categories of models: energy balance models, advective integral models and dynamic differential models. The analytical models generally require simplification of the equations describing the complex physical processes involved. Since these equations cannot be solved simultaneously, numerical techniques are used to produce approximate solutions. These generally involve convergence through a series of iterations, until predetermined criteria are met. All types of models require validation, and in the absence of well-documented high-quality data from field studies, this remains a major drawback of most urban climate models.

Todhunter and Terjung (1988) assessed the use of conventional meso-scale meteorological models to simulate urban conditions. This study found that the differences between predictions generated by such models and those generated by models that accounted for the urban geometry were substantial. Omission of geometry resulted in particularly large errors in the simulation of long wave radiant exchange. The authors concluded that urban canopy layer is too complex to be represented by modified 'plate models' (also referred to as 'slab models'), in which cities are modelled as an essentially homogenous surface, either soil or concrete, and surface properties such as the roughness length are modified to account for the three-dimensional character of the urban environment (Wieringa, 1993). However, such models are useful in evaluating the effect of major urban-rural differences, such as variations in soil moisture, on the properties of the boundary layer above roof height (Martilli, 2002).

In canopy layer models, the geometric complexity of real cities is simulated using computer models of synthetic cities, or representative parts of them. Many early models sought to simulate the three dimensional structure of cities (Terjung and O'rourke, 1980a; Terjung and O'rourke, 1980b). However, in spite of vastly increased computing power, subsequent computer models have found it more useful to simulate what is considered by many to be the basic unit of the built environment – the so-called urban canyon. This allowed the basic processes to be studied separately, including long wave radiation (Arnfield, 1982); short wave radiation (Verseghy and Munro, 1989); the surface energy balance (Arnfield *et al*., 1988; Arnfield, 1990; Sakakibara, 1996; Arnfield, 2000); and canyon air flow (Yamartino and Wiegand, 1986; Hunter *et al*., 1990-91; Macdonald, 2000). A recent model carries out a comprehensive two-dimensional simulation of wind, radiative exchange and storage (Herbert *et al*., 1998), while another is capable of three-dimensional analysis of the above parameters and in addition simulates the effect of vegetation on airflow (Bruse and Fleer, 1998). The evolution of air temperature in an urban canyon was modelled in a series of papers based on the concept of the Cluster Thermal Time Constant (CTTC), which expresses the thermal inertia of the urban physical structure (Swaid and Hoffman, 1990a; Swaid and Hoffman, 1990b; Swaid and Hoffman, 1990c; Swaid, 1993c).

In general, canopy layer models require numerous detailed inputs and are calculation-intensive; they are suitable for simplified geometries, such as symmetrical canyons; and most are limited to specific environmental conditions, such as clear skies and dry surfaces.

Coupling of the urban surface to a mesoscale atmospheric model may be done by two different methods (Taha, 1999):

- So-called '*slab models*' do not differentiate between the properties and behaviour of what are essentially very different surfaces, such as roads, building walls and roofs. In order to adjust for this simplification, the properties of the soil (e.g heat capacity, thermal conductivity) and surface albedo are modified to representative mean values for the urban ensemble, rather than simply representing real materials (Kusaka et al., 2001).
- The output from canopy layer models may be used as input to a meso-scale model to allow more accurate characterisation of the urban surface. This approach was adopted by Taha (1999), who incorporated the objective heat storage model (Grimmond et al., 1991) in place of the existing term for the soil heat flux to account for the micro-scale heterogeneity of the urban surface, thus modifying the CSUMM meso-scale model to apply to a city. However, it may be difficult to provide a sufficiently detailed description of the canopy layer of an entire urban area. The effort may in any case be redundant, because the detail will be lost when averaging inputs at a meso-scale grid (Taha and Bornstein, 1999).

A more detailed computational approach was developed by Masson (2000), who assessed three separate components of the urban energy budget to account for the differences between building walls, roofs and

roads. Like some of the urban canyon models, Masson's TEB model calculates surface temperatures to derive a detailed energy budget. However, since it aims to be applicable for meso-scale models, the grid mesh is larger than several hundred metres. At this scale, it was necessary to use average values for such variables as building height, street width etc., and street orientations are random. Evaluation of the TEB model using field observations from two relatively dry and sparsely vegetated urban areas with different morphologies suggests that this approach can produce good results (Masson *et al*., 2002), even though there were substantial discrepancies between measured and predicted fluxes.

A number of mesoscale models, such as Masson (2000) incorporate the effects of anthropogenic heat gains from building interiors by assuming a fixed interior air temperature and calculating conduction through a 'typical' wall section. A similar approach is adopted by Martilli *et al.* (2002), where computation of the surface temperature of building surfaces is carried out by solving a heat diffusion equation for a representative, multi-layered section where the inner-most layer is kept at a constant temperature. The contribution of energy generated by vehicles is usually treated as though it is injected directly into the air in the form of sensible heat, distributed evenly through the entire volume of the street canyon (Masson, 2000).

Meso-scale models are designed not only to model urban effects on temperature, but on dispersal of pollutants as well. Like models of air temperature, modelling airflow is carried out at different scales, beginning with the urban canyon, through entire cities (Martilli, 2003) and up to regional scale.

A problem common to all detailed analytical models is the coupling of fluxes from small-scale surface elements in the canopy layer to the roughness sublayer above and hence to the inertial (constant flux) layer.

The above models have a fine spatial resolution, and often require the evaluation of even smaller-scale components of the urban canyon system - e.g. the temperature of individual surfaces. At the opposite end of the spectrum of urban climate tools are models that deal with the whole city, albeit at a much lower resolution. Using such models, several researchers have attempted to assess the effect of various strategies to modify the microclimate of whole cities by means of extensive planting of trees or the widespread use of high-albedo materials on roof surfaces (Rosenfeld *et al.*, 1995; Taha *et al.*, 1997).

The advances in computing power and the development of geographical information systems (GIS) for organizing and displaying the spatial distribution of any desired property have led to the creation of detailed databases describing the urban surface on an ever more detailed scale. Cionco and Ellefsen (1998) presented a database developed for the city of Sacramento, which includes information on such parameters as building density, building height, roof reflectivity and plant cover on a grid of 100 metres by 100 metres. The use of such detailed information is perforce limited to simulation of the micrometeorological conditions in the specific location, but it gives an indication of the capabilities of existing meso-scale models.

Computational fluid dynamics (CFD)

Modelling of the urban environment may also be carried out by CFD, although this method is usually applied to environments of limited physical scale. The main difficulty that must be overcome is the description of

boundary conditions, which in a complex urban setting are often not known with sufficient accuracy. Unlike simpler methods, CFD requires that all relevant fluxes be calculated at the required scale in a full three-dimensional grid. In addition to requiring very detailed input, calculations require extensive computing resources, meaning models must be limited in space or simplified substantially. In both cases, calculation is limited to relatively short time periods, so the methodology is not applied to problems requiring time scales in excess of several days at most.

CFD modelling is used widely in qualitative studies of air movement and pollution dispersal in urban environments, the mechanics of which is still not fully understood (Chan *et al.*, 2001; , 2003). The effect on airflow in a hypothetical urban canyon of non-homogeneous heating of canyon surfaces by solar radiation was investigated by Xie *et al.* (2005). As expected, the strength of the canyon vortex was either enhanced or damped by thermal buoyancy, depending on whether the windward or leeward wall of the canyon was heated. This in turn has implications for the diffusion of scalars such as vehicle emissions (but also energy).

CFD modelling has also been used to investigate the effects of vegetation on microclimatic conditions in a city block (Dimoudi and Nikolopoulou, 2003). The study found that, as expected, evapotranspiration may reduce air temperature, especially if air speed is low. However, accurate prediction of meteorological parameters in the study area appears to have been impeded by an insufficiently long fetch or inadequate characterisation of boundary conditions upwind. This problem can be resolved by coupling simulation of microclimatic conditions in a CFD model with a simpler one-point model of meso-scale conditions (Bruse and Fleer, 1998), although this still requires appropriate inputs and does not solve problems that might result from variations in the three-dimensional morphology of the surrounding urban environment.

The accuracy of CFD simulations of a real urban environment was investigated by Takahashi *et al.* (2004) in a study of a group of buildings in Kyoto, Japan. Although the predicted temperatures of building surfaces and of the air 45 metres above the ground agreed closely with measured values, there were large errors in prediction of heat fluxes, which the authors were unable to explain but which were attributed to insufficiently accurate modelling of the finer features of the real buildings.

Statistical models

Simple regression of urban-rural climatic differences against one or more meteorological parameters is one of the oldest forms of urban modelling. It is easy to apply, requires no sophisticated software, but under certain conditions may provide some useful forecasts of basic urban climatological factors. The correlation found between maximum heat island intensity observed in a city and the canyon sky view factor is an example of the insight that may be gained through the application of such techniques (Oke, 1981).

Statistical models do, however, have several major drawbacks. First, they do not generally provide an explanation of the basic physical processes contributing to the urban microclimate. In order to be of any value, they need to be based on large and representative samples of data. Finally, they need to be calibrated using local data if the predictor equations are to provide useful results.

Digital elevation models

Digital Elevation Model (DEM) data files are digital representations of cartographic information in a raster form. DEMs consist of a sampled array of elevations for a number of ground positions at regularly spaced intervals. The technique, originally developed for study of landforms, has been applied to urban studies (Steemers *et al*., 1997; Ratti and Richens, 1999). The models may be used to analyse the effects of morphology on various urban properties, including sky view factors, shading and airflow. Application of this methodology was demonstrated in a study of the optimal building morphology for an arid climate (Ratti *et al.*, 2003). While the criteria for this particular study were rather limited, since the focus was on exposure to direct solar radiation and availability of daylight to the exclusion of such factors as ventilation, the technique shows much promise as a tool for investigating the effects of morphology. It does not, however, allow calculation of fluxes or simulate the actual physical processes that affect the urban microclimate.

3.2 The CAT Model

The CAT (Canyon Air Temperature) model is designed to allow prediction of a representative air temperature in an urban canyon on the basis of measured meteorological parameters from a reference station located at a nearby site exposed to the same meso-scale climatic conditions. The underlying assumption is that in the absence of differences between the sites, such as in their morphology or surface cover, microclimatic conditions in both sites would have been identical. Restrictions on the selection of the reference station will be discussed in detail in Chapter 7. It should be emphasised that the utility of the model depends on the availability of such reference data. Therefore, model inputs are limited to meteorological parameters monitored routinely at standard stations. This restriction has important implications that will be discussed in detail in the relevant sections below.

The traditional approach to numerical modelling of the microclimatic characteristics of the urban canopy layer has been a multi-layered one. Weather data are used to provide geographically-adjusted boundary conditions to a planetary boundary layer (PBL) model, such as URMICLEM (Taha, 1978). The meso-scale meteorological conditions predicted by this model, in conjunction with detailed site-specific descriptors, are used to drive an urban climate model capable of providing micro-scale temperatures at the site under consideration. This approach is based on a complete analysis of the energy fluxes, but requires climatic information that is generally not available at the detailed level required for the computer simulation.

The CAT model adopts a simpler approach: the raw weather data itself serves as the input to the urban climate model, sacrificing comprehensive analysis in the interests of practicality and ease of application. This approach was the basis of the modified CTTC computer code (Elnahas and Williamson, 1997), an analytical model incorporating a cluster thermal time constant for predicting air temperature variations in the urban canopy layer. Itself an extended version of a previous model originally proposed by Swaid and Hoffman (1990c), the extended CTTC model predicts air temperature at an urban site based on measured

temperature at a (rural) reference site, modified by the contribution of characteristically urban conditions. The conceptual basis for this conversion was stated by Elnahas and Williamson as follows:

$$T_a(t)_{urb} = T_b + \Delta T_{sol}(t)_{urb} - \Delta T_{lw}(t)_{urb} \quad (3.1)$$

$$T_a(t)_{met} = T_b + \Delta T_{sol}(t)_{met} - \Delta T_{lw}(t)_{met} \quad (3.2)$$

where $T_a(t)$ refers to air temperature at a given location, T_b the meso-scale base temperature, and ΔT_{sol} and ΔT_{lw} the net short wave and long wave radiative contribution to the local temperature. The subscripts '$_{urb}$' and '$_{met}$' refer to urban and meteorological (reference) locations, respectively. Combining the above expressions yields

$$T_a(t)_{urb} = T_a(t)_{met} + (\Delta T_{sol}(t)_{urb} - \Delta T_{sol}(t)_{met}) - (\Delta T_{lw}(t)_{urb} - \Delta T_{lw}(t)_{met}) \quad (3.3)$$

The above procedure attributes the variation in air temperature to differences in short wave and long wave energy balances between the urban site and the meteorological (reference) site. However, the same method may be employed to express differences resulting from other modifiers of local micro-climatic conditions, such as, for example, anthropogenic heat, the hydrological balance or the effects of vegetation, which may affect latent heat.

The CAT model adopts a similar conceptual approach, but employs a different methodology to compute the T_b, the meso-scale base temperature, and then to predict canyon air temperature. The process may be summarised as follows:

An energy balance is calculated from meteorological time series for the reference site and for each surface of the urban canyon, taking into account modifications to the energy exchange processes resulting from the specific characteristics of both sites. The microscale modification of air temperature at the reference site is calculated as the product of the sensible heat flux at the surface and a coefficient describing the resistance to turbulent heat transfer. This coefficient is derived from the surface heat exchange coefficient, modified by an empirical factor accounting for atmospheric stability and mechanical turbulence above the surface, normalised by the ratio of overall surface area of the site to its plan area. The time-dependent contribution of the local sensible heat flux to the air temperature at the reference site is then deducted from air temperature measured in a standard instrument screen to give T_b, the meso-scale base temperature. The same methodology is then used to calculate the ensemble contribution to the local canyon air temperature of sensible heat flux from all canyon surfaces, similarly modified by the resistance of the urban canyon site to turbulent heat transfer. This contribution is then added to the base temperature to give the predicted air temperature in the canyon.

Inputs required by the model comprise two separate categories:

- Time series describing meteorological conditions at the reference site, including the dry bulb temperature of the air, relative humidity, wind speed, global and diffuse solar radiation on a horizontal plane, and cloud cover.
- Site characteristics describing both the reference site and the urban site being simulated, including:
  - geographic location (latitude and longitude)
  - building geometry, including street canyon aspect ratio, building density and ratio of massive external walls to site area
  - material properties, including surface albedo and the coefficients of the objective hysteresis model (OHM) of thermal storage (Grimmond *et al*., 1991).
  - hydrological factors affecting the parcelling of turbulent heat flux into latent heat and sensible, including the coefficients of the LUMPS model by Grimmond and Oke (2002).

The geometric representation of the urban environment is two-and-a-half-dimensional: canyon dimensions are given only in cross-section (length in the direction of the main longitudinal axis is considered semi-infinite). However, treatment of in-canyon wind is fully three-dimensional, as is the incorporation of solar position in the computation of short-wave radiant exchange.

The model treats each of the following factors components of the heat balance as follows:

Radiative exchanges

Net radiation (Q^*) may be measured directly, but is not usually monitored in a standard meteorological station. Furthermore, net radiant exchange depends on the orientation of the relevant surface, its angle of tilt with respect to the horizon and its degree of exposure to direct solar radiation, to the sky and to other terrestrial surfaces. The CAT model therefore utilises more commonly available data - global solar radiation and diffuse solar radiation (both on an unobstructed horizontal surface) and cloud cover, all recorded at hourly intervals at the reference station. Net radiant exchange at the reference station and on each surface in the urban canyon is then calculated on the basis of solar geometry and the respective view factors of the participating surfaces. (Trigonometric expressions of the view factors are given in Appendix A.)

Several approximations were adopted in the calculation procedure:

a. The effect on radiant exchange resulting from differences in atmospheric turbidity between the reference site and the urban canyon due to urban air pollution etc. may be neglected.

b. Diffuse solar radiation is considered isotropic and is not affected by apparent solar position and elevation above the horizon.

c. Incoming long wave radiation ($L\downarrow$) is isotropic and independent of elevation and azimuth.

d. Terrestrial surfaces are assumed to be sufficiently rough that reflected radiation is isotropic (the Lambertian assumption).

e. Secondary reflections from canyon surfaces are neglected. The net effect of this assumption on the accuracy of the radiant exchange model depends on the albedo of the surfaces and on their sky view factor: the error is minimal when albedo is low and the canyon aspect ratio is high, since multiple reflections among surfaces with similar properties results in little net exchange. Likewise, if the canyon aspect ratio is very low, walls comprise a relatively small proportion of the envelope and secondary reflections are negligible because most of the reflected solar radiation is lost through the canyon top. Neglecting secondary reflections may result in unacceptable error only if canyon surfaces (including the street) are very light in colour (e.g. freshly whitewashed walls) and canyon aspect ratio is neither very high nor very low, resulting in substantial losses through the canyon top due to secondary reflections.

f. The model does not differentiate between rough opaque surfaces and smooth glazed ones: neither transmission to building interiors nor specular reflections are modelled. This may result in unacceptable errors if the proportion of glazed areas in building facades is high (Tsangrassoulis and Santamouris, 2003).

g. Net long wave exchange between canyon surfaces may be neglected.

h. View factors used were representative values calculated from the centre of the respective surfaces. The error resulting from this approximation is negligible (less than 5%) in the case of symmetric canyon sections, but may result in unacceptable errors in the case of highly asymmetrical canyons. However, the since airflow is also not modelled accurately in such configurations, the application of the CAT model is restricted to canyons in which the ratio of heights of opposite walls is less than 1:2.

Incoming direct normal (beam) solar radiation is calculated from measured global radiation and diffuse radiation, taking into account solar elevation. Beam radiation is then used to calculate the direct component on building surfaces, with respect to orientation and mutual shading by other canyon surfaces. The proportion of each surface exposed to direct radiation is calculated using a model that allows input of separate (different) values for each canyon wall. In addition, the height and setback of adjacent buildings may be input to account for obstructions created by buildings that are much taller than those forming the primary canyon perimeter, or for tower blocks constructed on a 'podium' that comprises the actual canyon walls. (See Appendix B for details on calculation of partial shaded areas.)

Canyon surfaces not exposed to direct solar radiation, including portions of exposed surfaces shaded by adjacent walls, are considered as being illuminated by diffuse radiation and by reflected radiation only, in proportion to the respective view factors for each of the source areas.

The time-dependent total solar radiant flux on the i_{th} canyon surface receiving reflected radiation from j other canyon surfaces is thus given by the following expression:

$$I(t) = I_{dir}(t)(1 - PSA(t)) + I_{dif}(t)\Psi_s + \sum_j I_{dir+dif}(t)\, j(1 - m_j)(\Psi_{i-j}) \quad (3.4)$$

where $I(t)$ is the mean hourly total solar radiation incident on the surface (W m^{-2}), PSA is the partial shaded fraction of the surface, $I_{dir}(t)$ the hourly mean unobstructed direct component of the solar radiation, $I_{dif}(t)$ the hourly mean unobstructed diffuse component of the solar radiation, $I_{dir+dif}(t)$ the combined direct and diffuse components of the solar radiation, Ψ the view factor between two surfaces, m_j the solar absorptivity of surface j (W m^{-2} K) and Ψ_s the mean sky view factor for a surface. Reflected radiation, as noted above, takes into account primary reflections only.

Incoming long wave radiation ($L\downarrow$) is calculated from the dry bulb temperature of the air and from atmospheric humidity for clear sky conditions via the empirical correlation proposed by Brutsaert (1982) for atmospheric emissivity,

$$\varepsilon_a = 1.24\left(\frac{e_a}{T_a}\right)^{1/7} \quad (3.5)$$

where e_a is the partial water vapour pressure of air (mb) and T_a air temperature (K). The partial water vapour pressure of air may be calculated from relative humidity and air temperature following the procedure set out in ASHRAE (1989).

Sky radiation is calculated using the Stefan-Boltzmann relationship

$$L\downarrow = \sigma\varepsilon_a T_a^{\,4} \quad (3.6)$$

where σ is the Stefan Boltzmann constant (5.67*10^{-8} W m^{-2} K^{-4}), ε_a is sky emissivity and T_a air temperature (K).

A correction factor incorporating the effect of clouds on $L\downarrow$ is applied following (Martin, 1989):

$$L\downarrow(n) = (1 + 0.0224n - 0.0035n^2 + 0.00028n^3)L\downarrow_{clear} \quad (3.7)$$

Compared with other empirical corrections for the effect of clouds, such as the one proposed by (Oke, 1987) (equations 2.11 and 2.12 above), this expression sacrifices accuracy for simplicity of application: it requires no information on cloud type, which may not always be available in standard meteorological records.

Calculating outgoing long wave radiation from terrestrial objects requires knowledge of surface temperature. Full analytical solutions of the surface temperature require *a priori* knowledge of the thermal properties of the material and either assume a constant temperature at a given depth below the surface (Best, 1998), in the case of soil, or a known interior air temperature, in the case of building walls. These are easily obtained for most common construction materials, such as concrete or asphalt, but are less well-defined for most soils.

Furthermore, changes in moisture content also affect the thermal properties of soils, so any calculation based on these data would require detailed time-series, a method of obtaining the appropriate values from other parameters, such as rainfall - or the use of fixed values that are accurate for only part of the time. The problems arising from the varying thermal properties of soil were noted by Oke (1998b) in the context of establishing a rural reference against which to evaluate urban effects on microclimate.

The approach adopted in the CAT model is a compromise between detailed modelling of surface temperature, which may give accurate results, and use of ambient air temperature as a surrogate for surface temperature, as proposed by Elnahas and Williamson (1997), which is less accurate but has the benefit of simplicity. In CAT, the temperature of a surface is approximated by its sol-air temperature.

The 'sol-air temperature' is defined as "the equivalent outdoor temperature which will cause the same rate of heat flow at the surface and the same temperature distribution throughout the material as results from the outdoor air temperature and the net radiation exchange between the surface and its environment" (Rao and Ballantyne, 1970). The commonly used notation has been modified to conform to conventions used in climatology, below:

$$T_{sol} = T_a + \frac{K\downarrow \alpha + \varepsilon_s L*}{h_c} \tag{3.8}$$

where T_{sol} is given in K, $K\downarrow$ is incoming short wave radiation (W m^{-2}), α is short wave absorptivity of the surface, ε_S is the long wave emissivity of the surface, $L*$ is net long wave radiation at the surface (W m^{-2}) and h_c the surface convective heat exchange coefficient (W m^{-2} K^{-1}). ε_S may be assigned separate values for each surface, but the model currently employs a value of 0.95 as the default. The outgoing long wave radiation ($L\uparrow$) is itself a function of the sol-air temperature, so its value is obtained by iterative calculation of the expression above until T_{sol} is obtained to an accuracy of less than 0.5K. The contributions of the ground surface and vertical surfaces of the canyon are calculated separately taking into account the appropriate view factors to the sky.

The main advantage of the sol-air temperature, which accounts for its widespread use in studies of bio-climatic design to describe the combined effect of air temperature and radiant exchange on a surface, is that it is invariant of the material of the surface in question, and can be calculated to a fair degree of accuracy from standard weather data together with the solar absorptivity and long wave emissivity of the surface. Unlike the Best model, however, the sol-air temperature cannot reproduce accurately the temperature of planted surfaces, since it does not model moisture flux. (See Section 6.4 for an experimental evaluation of the size of the error resulting from this approach.)

Heat storage (Q_S)

Heat storage is affected by the overall area of the surfaces exposed to the boundary layer and by their thermal properties. On the assumption that roof surfaces are not coupled directly to the urban canyon from a

thermal point of view, the active surfaces affecting conditions in the canyon are the floor and walls. The model treats each of these separately. It also assumes implicitly that ground surfaces are homogeneous and that all wall surfaces in the area being modelled are homogeneous, or that an average value may be used to represent them.

Heat storage described is modelled using the Camuffo and Bernardi (1982) formulation:

$$\Delta Q_s = a_1 Q* + a_2 \frac{\partial Q*}{\partial t} + a_3 \tag{3.9}$$

where t is time; the parameter a_1 indicates the overall strength of the dependence of the storage heat flux on net radiation; a_2 determines whether the curves ΔQ_S and $Q*$ are exactly in phase ($a_2=0$), or ΔQ_S precedes $Q*$ ($a_2>0$); a_3 is the size of ΔQ_S when $Q*$ becomes negative: a large value of a_3 indicates ΔQ_S becomes negative much earlier than $Q*$. Values of coefficients a_1, a_2 and a_3 correspond to typical values proposed by Grimmond and Oke (2002) for a variety of urban surfaces (see Table 2.4 above).

Turbulent heat flux (Q_H and Q_E)

The value of h_c, the surface convective heat transfer coefficient, is affected by the relative temperatures of the surface and the adjacent air layer, by the orientation of the surface with respect to the horizontal, and most importantly, by the speed of air movement across the surface. Since it cannot be determined by analytical methods, h_c is approximated by empirical correlations. Furthermore, since it is also affected by the turbulence characteristics of the flow, correlations obtained in wind tunnel experiments have not always proved satisfactory. The CAT model employs the following correlations, obtained experimentally on building surfaces at an urban site for horizontal and vertical surfaces, respectively (Hagishima and Tanimoto, 2003):

$$h_c = 3.96\sqrt{\overline{u^2 + v^2 + w^2}} + 6.42 \tag{3.10}$$

$$h_c = 10.2\sqrt{\overline{u^2 + v^2 + w^2}} + 4.47 \tag{3.11}$$

where u, v and w are wind vectors (m s^{-1}) and h_c is given in W m^{-2} K^{-1}.

In the reference site, wind speed near the surface is derived from measured data at 10-metre height, assuming a standard logarithmic profile. Values for the zero-plane displacement d and the roughness length z_0 are estimated from lookup tables assembled from numerous field experiments (Wieringa, 1993), in accordance with the aerodynamic characteristics of the site. In the case of a typical meteorological station, d is on the order of a few millimetres and z_0 about 1 centimetre. u_* can then be calculated using a value of k=0.4 for the von Karman constant:

$$u_* = k \frac{v_z}{\ln\left(\frac{z-d}{z_0}\right)} \tag{3.12}$$

Using the resulting value for u_*, the same expression is then solved for v_z to yield wind speed at the surface, taken as 20 centimteres, on the assumption that $(d+z_0)$ << 20cm.

The simple logarithmic profile is not appropriate in the urban canyon. Wind speed near canyon surfaces is calculated on the assumption that a vortex is formed, using the Hotchkiss and Harlow (1973) model, quoted in Yamartino and Wiegand (1986), to calculate wind speed near each of the surfaces from wind speed above the canyon top. The transverse (horizontal) component of the flow (u) and the vertical component (w) at any point in a two-dimensional rectangular notch of depth H and width B (in effect – an urban canyon) are given by the following expressions:

$$u = u_0(1-\beta)^{-1}\left[\gamma(1+ky) - \beta(1-ky)/\gamma\right]\sin(kx) \tag{3.13}$$

$$w = -u_0 ky(1-\beta)^{-1}[\gamma - \beta/\gamma]\cos(kx) \tag{3.14}$$

where $k=\pi/B$: $\beta=exp(-2kH)$; $\gamma=exp(ky)$; $y=z-H$; and u_0 is the transverse wind speed above the canyon (at the point $x=B/2$, $z=H$).

The transverse flow, which is independent of the along-canyon longitudinal flow, has a simple logarithmic profile:

$$v(z) = v_r \frac{\log\left[\frac{z+z_0}{z_0}\right]}{\log\left[\frac{z_r+z_0}{z_0}\right]} \tag{3.15}$$

where v_r is the along-canyon component of the wind speed at reference height r above the canyon and z_0 is the roughness length. In the absence of accurate local measurements, the roughness length is estimated as being one-tenth the average height of the canyon walls (Grimmond *et al*., 1998).

Yamartino and Wiegand (1986) note that the above model has two limitations:

- First, it assumes neutral atmospheric stability and height-independent shearing stress. In the context of the CAT model, inaccuracies may therefore result in unstable atmospheric conditions or in stable ones. However, the error in predicted wind speed is not likely to be substantial in most cases: In stable conditions, wind speed is generally very low, so even a large percentage error will result in a small absolute error; in unstable conditions buoyancy flows resulting from local inhomogeneities in surface temperatures will dominate only if mechanical turbulence is very weak.
- Second, z_0 has different values according to different angles of the approach flow with respect to the longitudinal axis of the street.

Sensible and latent heat flux are calculated for each canyon surface from the net radiant balance (Q*) and the storage flux (ΔQ_S) using the parameterisation proposed by De Bruin and Holtslag (1982), in the revised form given by Grimmond and Oke (2002) for urban conditions:

$$Q_H = \frac{(1-\alpha)+(\gamma/s)}{1+(\gamma/s)}(Q^*-\Delta Q_s)-\beta \tag{3.16}$$

$$Q_E = \frac{\alpha}{1+(\gamma/s)}(Q^*-\Delta Q_s)+\beta \tag{3.17}$$

where s is the slope of the saturation vapour pressure-versus-temperature curve; γ is the psychrometric constant; and α and β are empirical parameters. α depends on the soil moisture status, and accounts for the strong correlation of Q_H and Q_E with Q^*-ΔQ_S, whereas β accounts for the uncorrelated portion. Appropriate values for α must be selected according to surface type from the table shown in Grimmond and Oke (2002), which in turn is based on previous work by Hanna and Chang (1992) and Beljaars and Holtslag (1989, 1991). (See table 2.5 above).

Anthropogenic heat (Q_F)

In the CAT model, anthropogenic heat flux Q_F is added to the sensible heat flux Q_H before the temperature modification procedure is carried out. The energy is treated as if it is released homogeneously throughout the volume of the canyon.

Monthly mean values of total anthropogenic heat flux density are multiplied by a correction factor related to the time of day to adjust for the typical diurnal pattern of energy consumption, such as that observed by Sailor and Lu (2004).

Temperature prediction from sensible heat flux

The local effect of the sensible heat flux at the surface on air temperature in the canopy layer depends on the exchange of energy with the mixed layer above roof level, and is affected by two classes of factors (Kastner-Klein and Plate, 1999):

- The geometry of the urban canyon, especially its aspect ratio; and the morphology of the buildings it is defined by, especially the design of the roof. For a given canyon, the effect of these factors may be considered fixed over time.
- The characteristics of the airflow above the roofs, in particular wind speed and direction with respect to the canyon axis, and the magnitude of the turbulence. A further factor is the state of atmospheric stability near the surface. The effect of these factors changes constantly.

An accurate evaluation of this exchange may be carried out numerically by computational fluid dynamics (CFD). However, CFD requires very detailed input, and is still too demanding on computer resources to simulate extended periods. Analytical models, though less stringent in their requirements, nevertheless

require input of measurements sufficient to characterize atmospheric stability by parameters such as the Richardson number, which cannot be derived from typical meteorological station data.

An alternative method of accounting for the effects of atmospheric stability and mechanical mixing on turbulent flux was incorporated in CAT, whereby four separate classes of flow regimes were defined on the basis of the temperature difference between the sol-air temperature of the ground surface and the dry bulb temperature of the air at screen level. This temperature difference is a useful proxy for stability, since calculation of the sol-air temperature incorporates, in addition to air temperature, the meteorological factors that affect stability, namely radiant exchange (including the effects of cloud cover and air moisture content) and wind. Thus, the sol-air temperature can only be substantially below air temperature on clear nights with little or no wind; and it can only be much greater than the air temperature when the surface is exposed to intense solar radiation, if wind is light. The following table describes four classes of mixing regimes, using the sol-air temperature as an indicator of the combined effect of mechanical mixing and buoyancy flows, as described above:

Table 3.1: Definitions of mixing regimes between canopy layer and roughness sublayer

Mixing regime	Surface temperature depression (K)
Negligible mixing	<-2K
Light mixing	-2K<ΔT<0K
Moderate mixing	0K<ΔT<5K
Vigorous mixing	5K<ΔT

Each of the mixing regimes is characterized by a coefficient of turbulent exchange between the canyon and the mixed layer above roof height. This coefficient, designated m, may range in value between zero, corresponding to no mixing at all, and unity, corresponding to perfect mixing. The actual values used in the simulation were assigned empirically (See Chapter 6 below).

The exchange of sensible heat between the surface and the mixed layer above roof top height can be expressed by means of a bulk aerodynamic formulation for fluxes, of the general form:

$$Q_H = \Delta T / r \tag{3.18}$$

where Q_H is the sensible heat flux, obtained from the sum of the contributions of the individual surfaces comprising the envelope of the site, weighted by their respective areas as a proportion of the overall plan area of the site; ΔT is the temperature difference between the screen air temperature and the base temperature in the reference layer, which will vary over time; and r is a resistance to sensible heat exchange.

The value of r is given by the following expression:

$$r = (1-m) * r_{surf} \tag{3.20}$$

where r_{surf} is the resistance to sensible heat transfer at the surface and m is the coefficient of turbulent exchange.

The resistance to sensible heat transfer between canyon surfaces and the air (r_{surf}) is expressed as the inverse of h_c, the surface heat transfer coefficient in equations 3.10 and 3.11 above, normalised by the ratio of the total surface area of the site to its plan area (χ):

$$r_{surf} = \frac{1}{h_c * \chi} \tag{3.21}$$

Normalisation by χ is necessary because the increased surface area of the urban site results in more efficient heat transfer between the solid storage mass and the canopy layer air: The city, in its conceptual form as a series of urban canyons, in effect acts as a giant ribbed heat exchanger. Thus, the value of r_{surf} is lower for deep canyons than for shallow ones. In the event of a perfectly flat site, χ equals unity and equation 3.21 collapses into the familiar relationship where resistance is simply the inverse of conductance. The higher efficiency of heat transfer resulting from the increased surface area of urban sites is offset to a certain degree by the reduction in the magnitude of the surface convective coefficient, h_c, since wind speed near the surface of a street canyon is generally lower than in open sites.

The expression *(1-m)* accounts for differences in the rate of turbulent exchange at the canyon top due to mechanical mixing and thermal buoyancy. If either mechanism results in vigorous mixing of the air, m has a value approaching unity, *(1-m)* approaches zero and the effective resistance of the canyon system to exchange of sensible heat with the mixed layer above becomes negligible. If there is little mixing of the air, typically during strong thermal inversions, m has a much smaller value, *(1-m)* is proportionately larger and the product r_{surf} * *(1-m)* approaches the value of r_{surf}. In this case sensible heat exchange is limited to a shallow layer of air near the surface.

Finally, the time-varying change in air temperature resulting from the local characteristics the reference site and in the urban canyon, $\Delta Ta(t)_{met}$ and $\Delta Ta(t)_{urb}$ respectively, is obtained by solving equation 3.18 for ΔT separately for each of the two sites. The air temperature in the urban canyon $Ta(t)_{urb}$ is then calculated as the sum of the air temperature at the reference station $Ta(t)_{met}$ and the net change in temperature between the two sites:

$$T_a(t)_{urb} = T_a(t)_{met} + (\Delta T_a(t)_{urb} - \Delta T_a(t)_{met}) \tag{3.22}$$

In the current chapter, the canyon air temperature model has been described in abstract theoretical terms. The next chapter describes the detailed climate monitoring experiment carried out to establish empirical parameters incorporated in the model and to validate its accuracy.

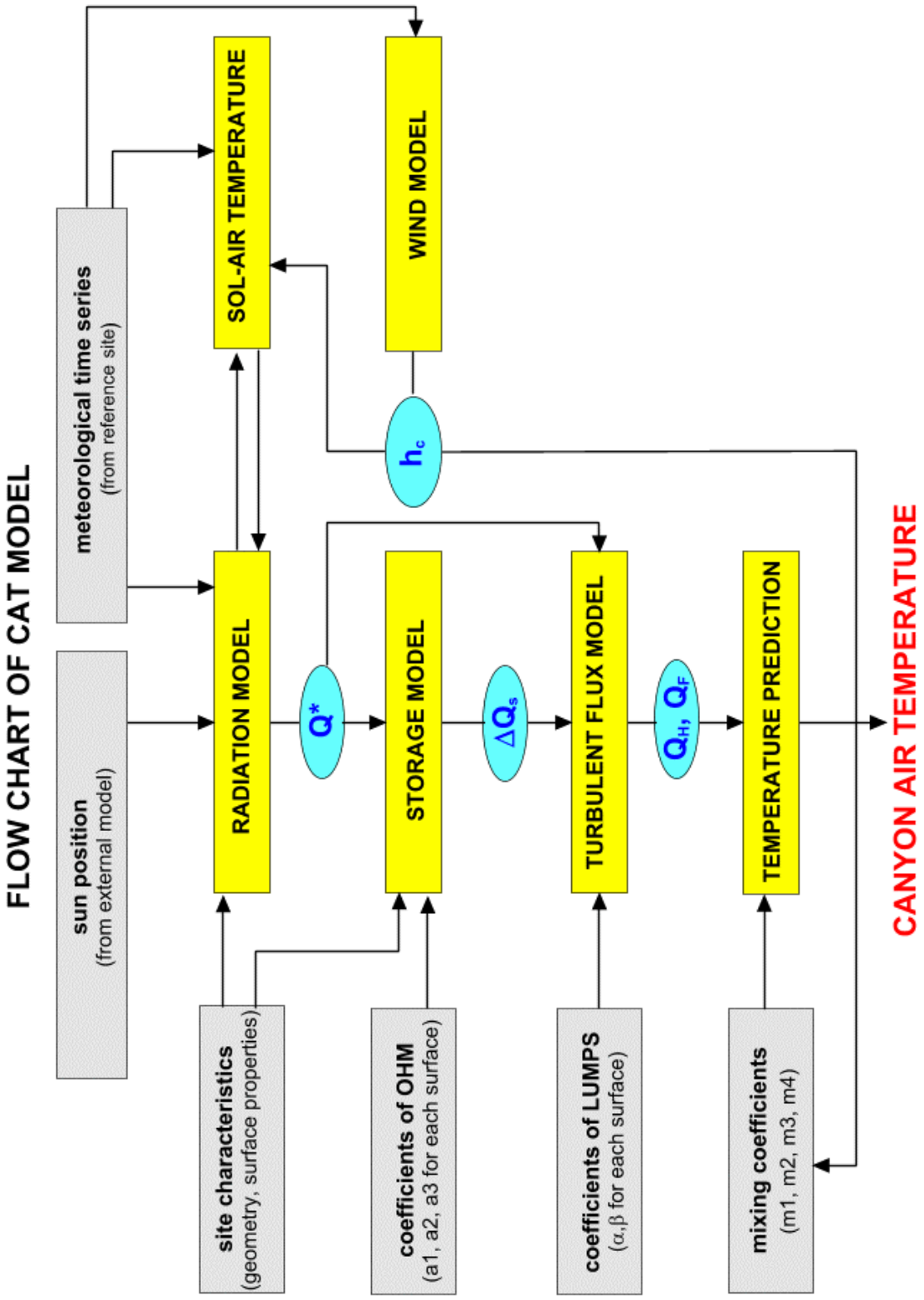

Figure 3.1: Flow chart of CAT model